

LEGENDRIAN KNOTS IN OVERTWISTED CONTACT STRUCTURES

Katarzyna Dymara*
Institute of Mathematics
Wrocław University

October 2004

ABSTRACT

We prove that two Legendrian knots in a contact structure which is trivializable as a plane bundle are Legendrian isotopic provided that (1) they are isotopic as framed knots, (2) they have the same rotation number with respect to some parallelization of the contact structure, and (3) there is an overtwisted disk disjoint with both knots. (For zero-homologous knots the condition (1) reads as: (1a) they are isotopic as topological knots, and (1b) they have the same Thurston-Bennequin invariant.) Then we discuss the situation when condition (3) is not fulfilled, in particular that of non-loose Legendrian knots.

0 Introduction

The present paper deals with Legendrian knots in overtwisted contact structures. In [4], the author proved (using Eliashberg's and Gray's theorems recalled here as Theorems 1.16 and 1.7 respectively) that two Legendrian knots in an overtwisted contact structure on S^3 disjoint with a fixed overtwisted disk are Legendrian isotopic if and only if they represent the same topological knot type and have equal values of invariants rot and tb (see Definition 3.1). The proof relies on homotopy considerations specific for S^3 , which makes it difficult to generalize to overtwisted contact structures on other manifolds.

In this paper we want to give a proof by direct manipulation on fronts, with the help of the idea (introduced by Fuchs and Tabachnikov in [12]) of following an arbitrary isotopy of knots by a Legendrian isotopy adding zig-zags whenever necessary. Because of those additional zig-zags, this method does not yield actual Legendrian isotopy, but only equivalence in the Grothendieck group of Legendrian knots (with the connected summation as the group operation). As it turns out, in the presence of an overtwisted disk an operation functionally identical to adding zig-zags can be performed by Legendrian isotopy. There is a clear advantage to this approach: one can fairly easily construct actual isotopies of Legendrian knots following the steps of the proof of Theorem 4.1 (the isotopies given as examples in Section 2 have been found this way), which would be rather problematic with the methods of [4]. On the other hand, comparing the two proofs suggests some sort of

* Partially supported by KBN grant 2 P03A 017 25.

connection between Fuchs and Tabachnikov's idea of Legendrian knot stabilization and the notion of overtwistedness, which may be interesting in itself.

The paper is organized in the following way. Section 1 recalls definitions and known facts on contact structures, and fixes notation to be used throughout the paper. In Section 2 we turn attention to Legendrian knot, again restating known results and adapting them to the situation of an overtwisted contact structure on S^3 ; this process continues throughout Section 3, but with respect to the classical invariants. Section 4 formulates and proves the main theorem (Theorem 4.1). Finally, in (somewhat eclectic) Section 5 we display several supposedly interesting examples of Legendrian knots, including many non-loose ones, and give a few classification results.

1 Contact Structures

A *contact structure* on a 3-dimensional manifold is a field of planes defined (at least locally) as the kernel of a 1-form α such that $\alpha \wedge d\alpha$ nowhere vanishes.

Example 1.1. The contact structure $\zeta = \ker(\alpha)$, where $\alpha = dz - x dy$, is called the standard contact structure on \mathbf{R}^3 .

Example 1.2. The contact structure $\zeta' = \ker(\alpha')$, where $\alpha' = \cos x dz - \sin x dy$, is isomorphic to ζ of Example 1.1 via the diffeomorphism

$$f_1 : \mathbf{R}^3 \rightarrow \mathbf{R}^3 : (x, y, z) \mapsto (xy \cos x + z \sin x, xy \cos x - y \sin x + xz \sin x + z \cos x).$$

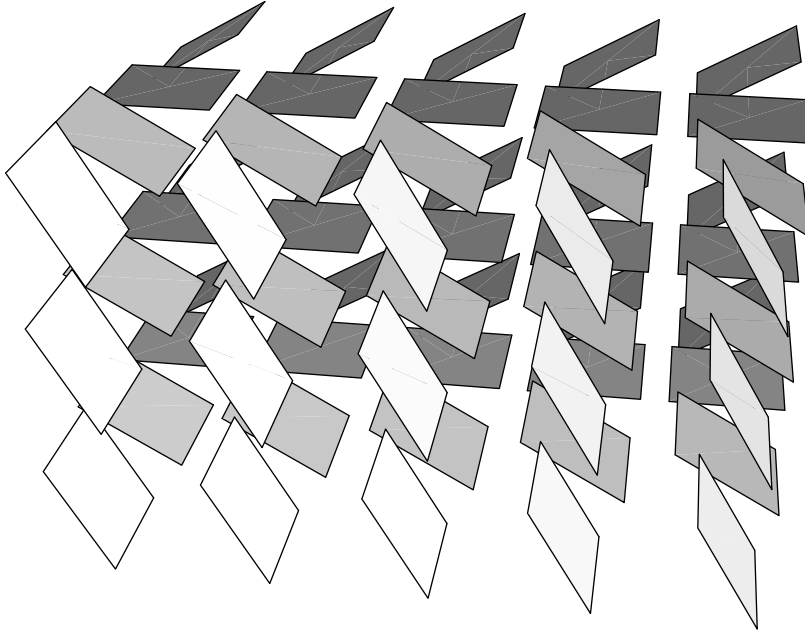


Figure 1: The standard contact structure ζ .

We say that two contact structures $\zeta = \ker \alpha$ and $\xi = \ker \beta$ on a manifold M are *isomorphic* if there exists a diffeomorphism $f : M \rightarrow M$ such that $f^*(\alpha) = t\beta$ for some non-zero function $t : M \rightarrow \mathbf{R}$.

In general, it is true that all contact structures look alike *locally* (but not globally, cf. Example 1.4); to be precise, in contact topology holds an analogue of the well-known (in symplectic setting) Darboux's Theorem.

Theorem 1.3 (Darboux's Theorem). *In any contact manifold any point has a neighborhood U contactomorphic to the standard contact structure ζ (see Example 1.1) on \mathbf{R}^3 .*

(For both the symplectic Darboux's Theorem and its contact version, consult for example Arnold's book [1].)

Example 1.4. The contact structure ξ on \mathbf{R}^3 , defined as the kernel of the 1-form (in cylindrical coordinates) $\beta = \cos r dz - r \sin r d\theta$, is not isomorphic to the contact structure ζ of Example 1.1. (Essentially, what distinguishes ξ from ζ is its property of being *overtwisted*, to be explained in Definition 1.11 and the discussion following it.)

Apart from the relation of isomorphism, there is another (equally natural, one would say, though possibly weaker) equivalence relation on the space of contact structures on a given manifold, namely that of isotopy (homotopy through contact structures).

Definition 1.5. We say that two contact structures ζ_0 and ζ_1 are *isotopic* if there exist a smooth family of contact structures $\{\zeta_t, t \in [0, 1]\}$.

An easy argument shows that on \mathbf{R}^3 all contact structures are isotopic. For ξ a contact structure, let ε be such that $\xi|_B$, where $B = B_\varepsilon(0)$, is isomorphic to the standard contact structure ζ (see Example 1.1). Then the family of pull-backs of ξ by maps f_t , which gradually shrink the entire \mathbf{R}^3 so that finally it falls into the ball B , provides an isotopy between ξ and ζ : for

$$f_t : \mathbf{R}^3 \rightarrow \mathbf{R}^3 : x \mapsto \left(\frac{\varepsilon}{t\|x\| + 1} \right) x \quad \text{and} \quad \xi_t = f_t^*(\xi)$$

we have $f_0 = \text{Id}$, so that $\xi_0 = \xi$, and $f_1(\mathbf{R}^3) = B$. Therefore ξ_1 is isomorphic to the standard ζ .

The situation is quite different in the case of closed manifold: Gray proved in [13] that the relation of isotopy is as strong there as that of isomorphism.

Theorem 1.6 (Gray's Theorem¹). *Given a smooth family $\{\zeta_t, t \in D^n\}$ of contact structures on a closed manifold M and a point $t_0 \in D^n$, there exists a family $\{\phi_t, t \in D^n\}$ of diffeomorphisms $\phi_t : M \rightarrow M$ such that for all t , $\phi_t^* \zeta_t = \zeta_{t_0}$.*

Throughout the paper, we will happily make use of this theorem, calling two contact structures “isomorphic” (or simply “the same”) as soon as an isotopy between them has been established.

¹ Actually, the original Gray's formulation goes along more telling and easy to remember lines: *Families of contact structures are locally trivial* (Theorem 5.2.1 in [13]).

Gray's proof (which uses a vector field whose flow consists of the desired diffeomorphisms, constructed locally and glued together by means of a partition of unity) can be applied—without essential changes—to a relative situation, either in the sense of considering contact structures on a manifold modulo a compact set, or fixing the contact structure along a (contractible) subset of the parameter space. Here we will simply reformulate Gray's theorem in a way as general as it is needed.

Theorem 1.7 (Gray's Theorem, relative version). *Let M and ζ_t be as in Theorem 1.6. Assume that $\zeta_t|_A = \zeta_{t_0}|_A$ for a compact set $A \subset M$ and for all $t \in D^n$. Moreover, let $\zeta_t = \zeta_{t_0}$ for all $t \in D'$, where D' is a contractible subset of D^n . Then there exists a family $\{\phi_t, t \in D^n\}$ of diffeomorphisms $\phi_t : M \rightarrow M$ such that for all t , $\phi^*\zeta_t = \zeta_{t_0}$, for all $t \in D^n$ $\phi_t|_A = \text{Id}_A$ and for all $t \in D'$ $\phi_t = \text{Id}_M$.*

This is just one of the reasons why in the present paper we prefer to discuss contact structures on a closed manifold. Since all the basic examples described above happened to be contact structures on \mathbf{R}^3 (due to the ease with which to set a coordinate system on the euclidean space), we will make up for this one-sided approach by providing a spectrum of examples sitting on the 3-sphere.

In order to accompany these examples by an illustrative figure, let us employ the following way of looking at S^3 .

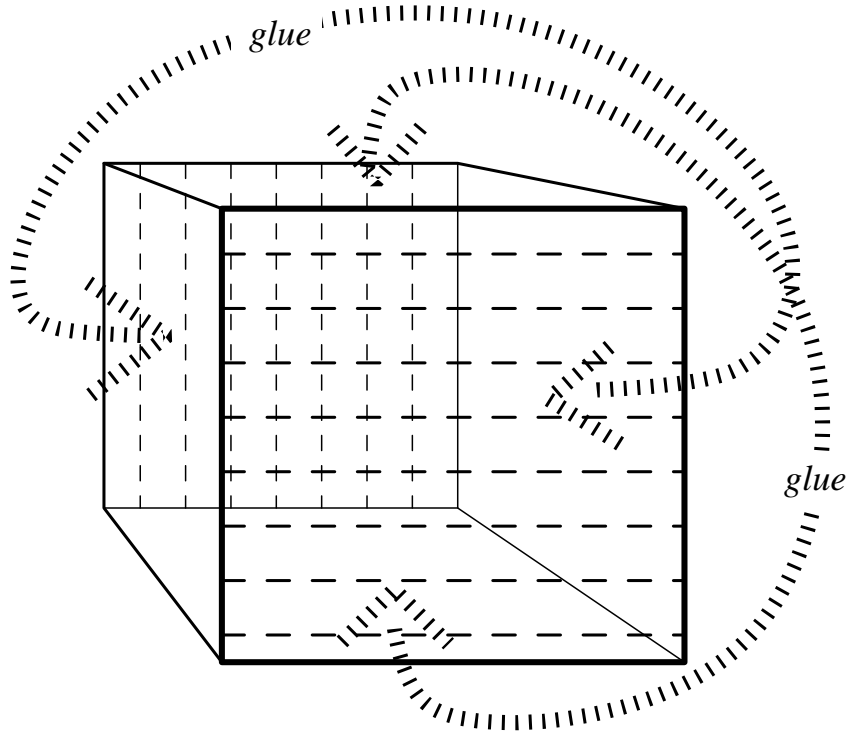


Figure 2: Gluing of the cube (Construction 1.8).

Construction 1.8. Consider the cube $\mathcal{C} = [0, 1] \times [0, 1] \times [0, 1]$. Identify two points (x, y, z) and (x', y', z') in \mathcal{C} if any of the following condition holds:²

- (a) $x = x', y = y', z = 0, z' = 1$, or
- (b) $x = x', y = 0, y' = 1, z = z'$, or
- (c) $x = x' = 0, z = z'$, or
- (d) $x = x' = 1, y = y'$.

Then the quotient is homeomorphic to S^3 . We will denote the projection map $\mathcal{C} \rightarrow S^3$ by $\text{pr}_{\mathcal{C}}$.

This construction provides a system of coordinates on the 3-sphere, which can be used to write explicitly 1-forms defining certain contact structures.

Example 1.9. For any integer $n \geq 0$, let the contact structure ζ_n on S^3 be the kernel of the 1-form $\alpha_n = \cos((n + 1/2)\pi x) dz - \sin((n + 1/2)\pi x) dy$.

Note that for each n the form $\alpha_n = dz$ on the front face $\{x = 0\}$ and $\alpha_n = \pm dy$ on the back face $\{x = 1\}$. Thus all ζ_n 's are indeed well-defined contact structures on S^3 . Now let us have a closer look at one of them.

Example 1.10. The contact structure ζ_0 (defined as above with $n = 0$) is known as the standard contact structure on S^3 . It can be described independently of Construction 1.8 as the field of planes perpendicular to the fibers of the Hopf bundle. Removing a point from (S^3, ζ_0) yields a contact structure on \mathbf{R}^3 isomorphic to ζ from Example 1.1.

Each of the contact structures described in Example 1.9 belongs to one of exactly three different isomorphism classes. It is easy to notice that, considered as plane fields, all ζ_n 's with n odd realize one homotopy type, those with n even—another one. But in addition to that, ζ_0 can be proved to be different from ζ_2 ($\simeq \zeta_4 \simeq \dots$) using the notion of overtwistedness (introduced in [2]).

Definition 1.11. Let $R = [0, 2/3] \times [0, 1] \times \{z_0\} \subset \mathcal{C}$ for some z_0 , $\Delta = \text{pr}_{\mathcal{C}}(R)$ in S^3 with the contact structure ζ_1 of Example 1.9. A 2-dimensional disk D in a contact manifold (M, ξ) is an *overtwisted* disk if it has a neighborhood contactomorphic to a neighborhood of Δ . A contact structure (or contact manifold) is called *overtwisted* if there is an overtwisted disk in it.

Example 1.12. Let $R' = [1/3, 1] \times \{y_0\} \times [0, 1] \subset \mathcal{C}$ for some y_0 . The disk $\text{pr}_{\mathcal{C}}(R')$ is another overtwisted disk in (S^3, ζ_1) .

Example 1.13. For each z_0 , the disk $\Delta_{z_0} = \{(r, \theta, z) \mid r \leq \pi, z = z_0\}$ is an overtwisted disk in (\mathbf{R}^3, ξ_0) for ξ_0 defined as in Example 1.4.

Definition 1.14. A contact structure which is not overtwisted is called *tight*.

² In more informal language we would say: glue together the left and right faces of the cube, and also the top and bottom faces; then contract to points all horizontal lines on the front face, and also all vertical lines on the back face. Cf. Figure 2.

Example 1.15. The contact structure ζ (and ζ') on \mathbf{R}^3 described in Examples 1.1 and 1.2, as well as ζ_0 on S^3 from Example 1.10, are tight.

The tight-vs-overtwisted dichotomy has unexpectedly deep consequences. Results obtained and methods useful in studying overtwisted contact manifolds have very little in common with those appropriate for tight ones. The classification results for tight contact structures are rather mysterious: not universal but proved on a manifold-by-manifold basis ([14], [15], [7]), often surprising ([8]) and refer to a rich hierarchy of notions of fillability (cf. the discussion of Question 1 in [10]). In the case of overtwisted contact structures virtually all that has ever been said about classification is contained in one powerful (though deceptively simple in formulation) theorem of Eliashberg [5].

Theorem 1.16 (Eliashberg’s Theorem). *For Δ a 2-dimensional disk in an arbitrary 3-manifold M , let ξ_Δ be a contact structure on a neighborhood of Δ for which Δ is an overtwisted disk. Denote by $\text{Cont}_\Delta(M)$ the space of contact structures on M which coincide with ξ_Δ on a neighborhood of Δ . Moreover, let $\text{Distr}_\Delta(M)$ be the space of all plane distributions on M which coincide with ξ_Δ on a neighborhood of Δ . Then the natural embedding $\text{Cont}_\Delta(M) \rightarrow \text{Distr}_\Delta(M)$ is a weak homotopy equivalence.*

On π_0 level this means that isotopy classes of contact structures overtwisted along a fixed disk (which, since embeddings of a disk into a connected manifold are all isotopic, actually exhaust all isotopy classes of overtwisted contact structures) remain in a one-to-one correspondence with homotopy classes of plane fields.

For S^3 , which is our main object of interest, co-oriented³ plane fields can be identified with maps into S^2 by means of fixing a parallelization (a trivialization of the tangent bundle). Therefore, the space of overtwisted contact structures is parameterized by the set $\pi_0(\text{Map}(S^3 \rightarrow S^2)) = \pi_3 S^2 \simeq \mathbf{Z}$.

2 Legendrian Knots

Now we turn attention to Legendrian knots. In this section (with its multitude of figures) we introduce a device, analogous to front diagrams in the standard tight contact structure, but suitable for studying Legendrian knots in overtwisted contact structures on S^3 (Construction 2.1), display several examples, and prove a(n appropriate version of) theorem about Reidemeister moves.

A curve in a contact 3-manifold tangent to the contact planes at each point is called *Legendrian*. The term *Legendrian knot* is usually applied to a Legendrian curve which is a knot, i.e. an embedding of the circle.⁴

³ Of course, all plane fields on S^3 (or any manifold with trivial H_1) are co-orientable; we consider them as pre-equipped with one of the two possible co-orientations simply as a matter of convenience.

⁴ In [12], Fuchs and Tabachnikov refer to such a curve (in the standard tight contact

We say that two Legendrian knots are *Legendrian isotopic* if they are isotopic via Legendrian knots; this is an equivalence relation. The words “Legendrian knot” are often used to mean a Legendrian knot *type*, i.e. a class of Legendrian isotopy.

We will also make extensive use of *knot diagrams*, i.e. projections of knots on a plane (or a surface) in general position.

Projections of Legendrian knots in (\mathbf{R}^3, ζ) on the yz plane yield their so called *front diagram*. Those are plane curves which are never vertical and may have—despite the knot being in general position—cusp singularities. Fronts are easier to manipulate, since there is no metric condition involved, and provide a comfortable tool for studying Legendrian isotopies. Two Legendrian knots are Legendrian isotopic if and only if there is a homotopy between their front diagrams which is an isotopy except for finitely many points, where one of the *Legendrian Reidemeister moves* (recalled on Figure 5) occurs [18].

In the present paper we will employ a device similar to front diagrams in \mathbf{R}^3 , but better suited to the contact manifold of our interest.

Construction 2.1. (*Fronts on the torus, fronts on the cylinder.*) Consider S^3 with the contact structure ζ_1 as in Example 1.9. Recall Construction 1.8; the images of the front and back faces are two linked circles. A Legendrian knot K in general position is disjoint with those circles, i.e. $\text{pr}_{\mathcal{C}}^{-1}(K)$ lies in $\mathcal{C}_0 = (0, 1) \times [0, 1] \times [0, 1]$. Let $p : \mathcal{C}_0 \rightarrow \{0\} \times [0, 1] \times [0, 1]$ be the orthogonal projection; since $\text{pr}_{\mathcal{C}}$ is injective on \mathcal{C}_0 , $P = \text{pr}_{\mathcal{C}} \circ p \circ \text{pr}_{\mathcal{C}}^{-1}$ is well-defined and $P(K)$ is a curve on the torus $T^2 = \text{pr}_{\mathcal{C}}(\{0\} \times [0, 1] \times [0, 1])$, smooth except for possible cusp singularities. We will refer to $P(K)$ as the *front diagram* of K on the torus.

Note that \mathbf{R}^3 with the contact structure ξ of Example 1.4 is contactomorphic to the open subset $\text{pr}_{\mathcal{C}}([0, 1) \times [0, 1] \times (0, 1))$. Thus a Legendrian knot in (\mathbf{R}^3, ξ) can be diagrammatically represented by a front on the torus never crossing a fixed meridian of the torus (i.e. the image of the top and bottom faces of the cube); such a curve may be called a *front on the cylinder*.

Moreover, let Δ be an overtwisted disk in a contact manifold (M, ζ) . A small neighborhood of Δ is contactomorphic to a neighborhood of the standard overtwisted disk in (S^3, ζ_1) (by the standard overtwisted disk in (S^3, ζ_1) we understand $\text{pr}_{\mathcal{C}}^{-1}(R)$ for $R = [0, 2/3] \times [0, 1] \times \{z_0\} \subset \mathcal{C}$; cf. Example 1.12). Therefore Legendrian curves in this neighborhood can also be represented by fronts on the cylinder.

It is not the case that every curve on the torus is the projection of a Legendrian knot. Knot diagrams on the torus satisfy a condition analogous to—though more complicated than—that of front diagrams being never vertical.

For $n \geq 1$, a curve of any slope can be the projection of a Legendrian curve in ζ_n . Moreover, for some slopes there is an ambiguity in determining the x coordinate of the original curve. Indeed, the contact structure ζ_1 looks exactly the same at (x, y, z) as at

structure on \mathbf{R}^3) as a *short* Legendrian knot, with the term *long Legendrian knots* reserved for Legendrian embeddings of \mathbf{R} coinciding with the y axis outside of a compact set; one can broaden the notion of a long Legendrian knot to include any proper Legendrian embedding of \mathbf{R} (with fixed behavior in the infinity) into an open contact manifold. All the results of this paper are valid for long as well as short Legendrian knots, unless otherwise specified.

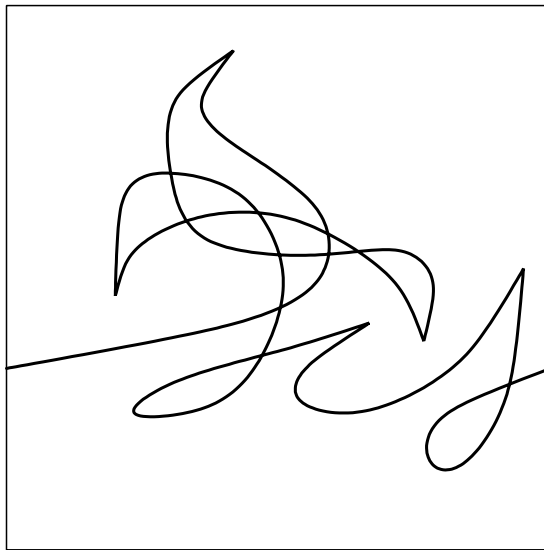


Figure 3: A front on the torus (which can be interpreted as a front on the cylinder).

$(x + 2/3, y, z)$; and generally: ζ_n looks exactly the same at (x, y, z) as at $(x + 2/(2n+1), y, z)$. Thus locally any curve in the torus lifts to n or $n+1$ different curves in (S^3, ζ_n) . However, once a starting point has been chosen, the Legendrian lift has to be continued in a unique way; and it may happen that a particular curve cannot be lifted. Below we formulate the necessary and sufficient conditions for a curve on the torus to be the projection of a Legendrian knot.

Proposition 2.2. *Let $k : S^1 \rightarrow T^2$ be a curve in the torus, $g_k : S^1 \rightarrow RP^1$ its tangent Gauss map.⁵ Let $p : \mathbf{R} \rightarrow RP^1$ (of period π) be the universal covering map of RP^1 . The curve k is the projection of a Legendrian knot in ζ_n if and only if*

- (i) g_k lifts to a map $\tilde{g}_k : S^1 \rightarrow \mathbf{R}$, where $g_k = p \circ \tilde{g}_k$; and
- (ii) $\text{im}(\tilde{g}_k) \subset (\ell\pi, (\ell + n + 1/2)\pi)$ for some $\ell \in \mathbf{Z}$.

Proof: Assume that the curve k is the projection of a Legendrian knot K , where $K(t) = (x_K(t), y_K(t), z_K(t))$. The Gauss map g_k must agree with the x coordinate of K , i.e. as \tilde{g}_k we can choose $3/2\pi x_K(t)$. But $\text{im}(x_K) \subset (0, 1)$, so the condition (ii) is satisfied.

On the other hand, when $\text{im}(\tilde{g}_k) \subset (\ell\pi, (\ell + n + 1/2)\pi)$, take $x_K(t) = \tilde{g}_K(t) - \ell\pi$. \square

Even for $n = 1$ we can notice that the intervals $(\ell\pi, (\ell + 3/2)\pi)$ are not pairwise disjoint. This is connected with the ambiguity in determining the x coordinate discussed above. If the image of \tilde{g}_k is contained in the interval $(0, \pi/2)$ —as it is, for instance, for the flying saucer of Figure 8(b)—then k is the diagram of each of two distinct Legendrian knots in ζ_1 , one of which lies entirely in the front $1/3$ of the cube, and the other one in the back $1/3$. However, the difference of the values of \tilde{g}_k (or the x coordinates) at two given points on a knot is always uniquely determined. This observation will play an important role in Proposition 2.4.

⁵ We take it to have the codomain in RP^1 rather than S^1 so that we don't have to fix an orientation of k .

Example 2.3. A curve on the torus of constant slope m/n (see Figure 4) is the diagram of a Legendrian knot in ζ_1 , which we will denote $\Gamma_{m,n}$. If $mn \leq 0$, then $\Gamma_{m,n}$ is uniquely determined; otherwise, there are two possibilities. For example, $\Gamma_{0,1}$ and $\Gamma_{1,0}$ have diagrams consisting of (respectively) a horizontal and a vertical line segment. They are boundaries of overtwisted disks described in Definition 1.11 and Example 1.12.

Fronts on the torus may be used in studying Legendrian isotopies of knots, in a similar way as Świątkowski in [18] used the usual front diagrams for knots in the standard tight contact structure on \mathbf{R}^3 . The following result is analogous to his Theorem B.

Proposition 2.4. *Two fronts on the torus are projections of Legendrian isotopic knots if and only if we can pass from one to the other by a finite sequence of moves of the following types:*

- (0) *an isotopy of the fronts;*
- (I) *the type I Reidemeister move (the dovetail move), see Figure 5(I);*
- (II) *the type II Reidemeister move in two versions:*
 - (a) *in the presence of a cusp, see Figure 5(II), and*
 - (b) *without a cusp (see Figure 6), but under the assumption that the x coordinates of both strands differ by at least π ;⁶*
- (III) *the type III Reidemeister move, see Figure 5(III); and*
- (IV) *the move changing the homotopy class of the diagram (see Figure 7) by passing through*
 - (a) *the front face of the cube, or*
 - (b) *the back face.*

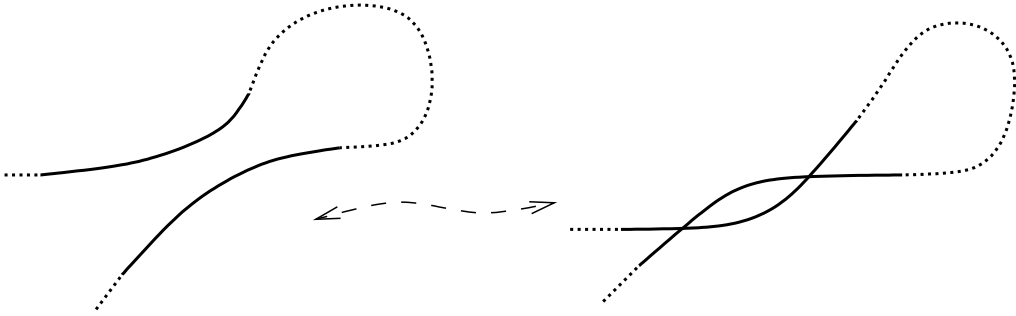
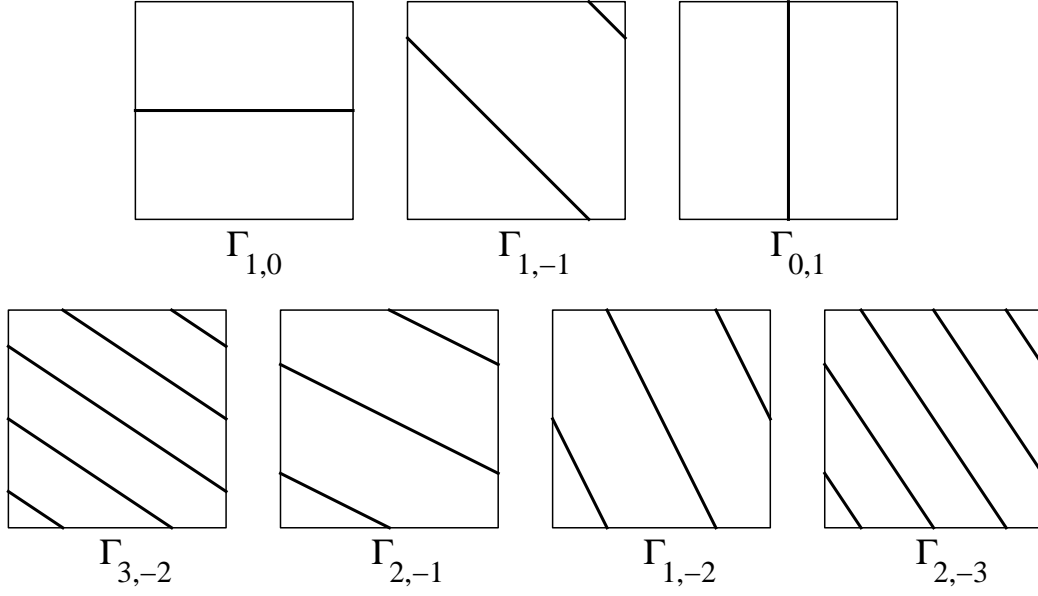


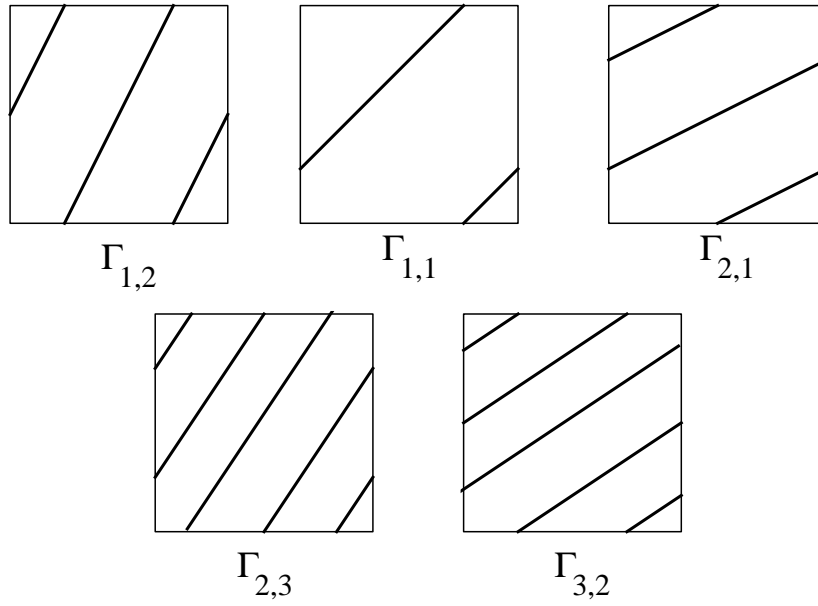
Figure 6: The type II Reidemeister move without a cusp.

Proof: As one would expect, this statement may be derived from (a refined version of) the transversality theorem. Details of the reasoning are very similar to those given by Świątkowski in [18], with just a few changes. The euclidean space \mathbf{R}^3 needs to be replaced with S^3 , and the plane Q —with the torus T . The possibility of a nontransversal self-intersection of the diagram (cf. [18], p.203) is no longer excluded; the projection of a Legendrian knot

⁶ This condition has been symbolically depicted in Figure 6 by joining the strands with a dotted line which makes a U-turn before returning to the point where the move is performed; of course, the actual diagram may look different.



(a) the uniquely determined $\Gamma_{m,n}$'s



(b) the ambiguous $\Gamma_{m,n}$'s

Figure 4: The knots $\Gamma_{m,n}$.

on the torus may have self-tangencies, provided that the condition of (IIb) is satisfied. Such a self-tangency yields the move of Figure 6.

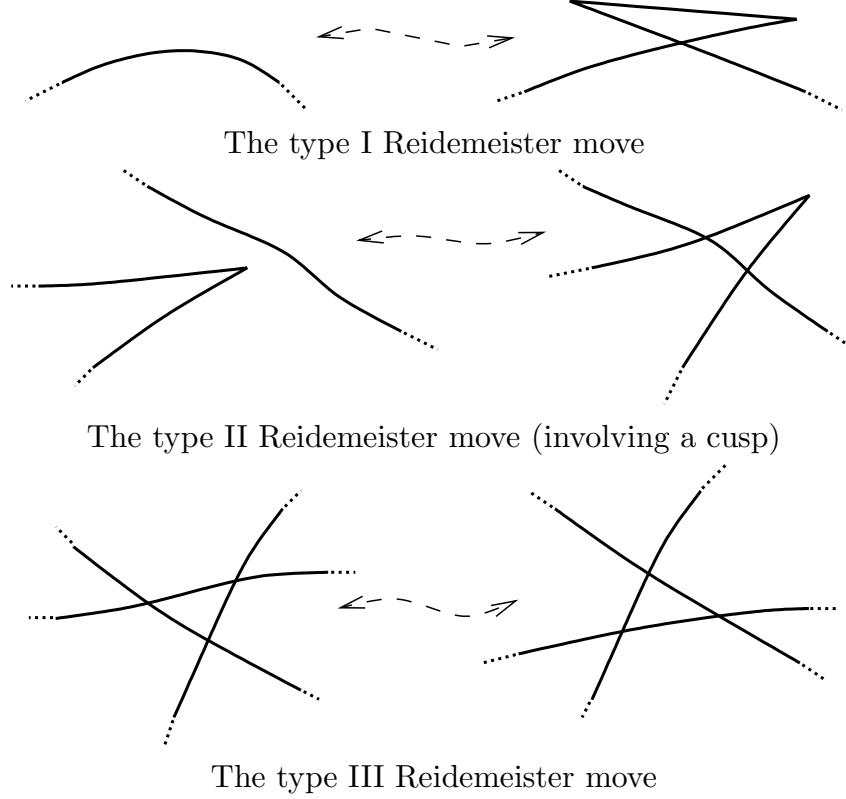


Figure 5: The local Legendrian Reidemeister moves (cf. [18]).

Furthermore, in Świątkowski's Definition 3.2 we require an additional transversality condition, namely that the isotopy $H : S^1 \times I \rightarrow S^3$ is transversal to $c_f \cup c_b \subset S^3$. It implies that, if $H(S^1, t) \cap c_f \neq \emptyset$ for a given t , then a move of type (IVa) takes place at t , and analogously for $H(S^1, t) \cap c_b \neq \emptyset$ we have a move of type (IVb). \square

Example 2.5. The four Legendrian (un)knots depicted on Figure 8 are Legendrian isotopic.

Example 2.6. The two knots depicted at the top of Figure 9 are Legendrian isotopic. Note that these knots considered as Legendrian knots in the standard tight contact structure (known as *the Chekanov examples*) are not Legendrian isotopic.

For a manifold M with a co-oriented contact structure ξ the contact embedding

$$j : (\mathbf{R}^3, \zeta_0) \hookrightarrow (M, \xi)$$

is unique up to isotopy, because any such embedding can be isotoped to one with the image in an arbitrarily small ball. When $M = S^3$ and $\xi = \zeta_1$, we get the front diagram of $j(K)$ simply transferring the diagram of K to the torus without any change of shape. Of course, the image of a Legendrian isotopy is still a Legendrian isotopy; thus j induces a map

$$j_* : \{\text{Legendrian knot types in } \zeta_0\} \rightarrow \{\text{Legendrian knot types in } \xi\}.$$

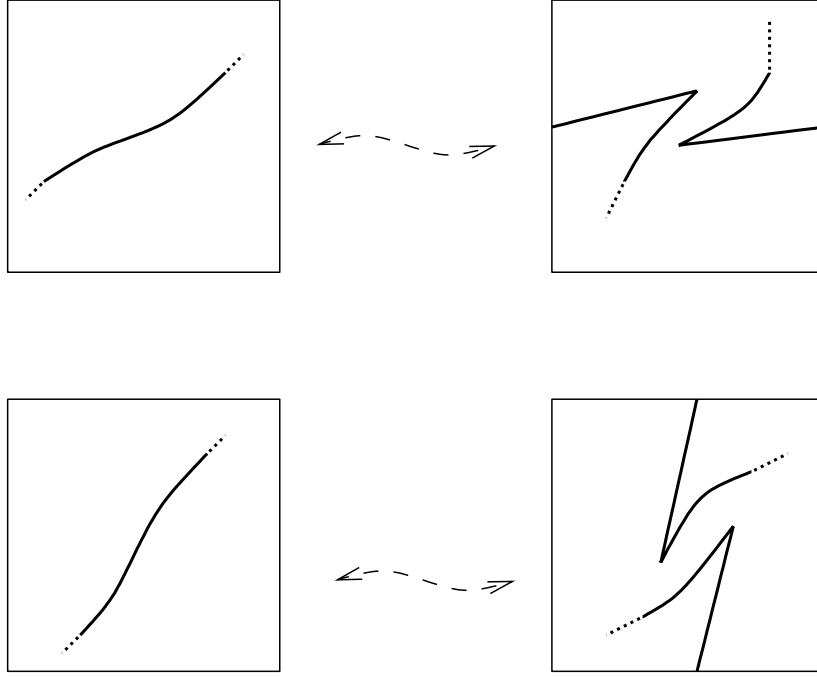


Figure 7: The moves through the front/back faces.

Example 2.6 shows that this map does not have to be injective. Neither is it necessarily surjective; in the following we will call a Legendrian knot *standard* if it lies in the image of j_* .

3 The Classical Invariants

Now we recall the definitions of two classical (integer-valued) invariants of Legendrian isotopy of knots, the *rotation* (or Maslov) number and the *Thurston-Bennequin* invariant. They were first introduced by Bennequin in [2], and since then has been widely used for Legendrian knots in the standard tight contact structure on \mathbf{R}^3 (or S^3). As we are mainly interested in overtwisted contact structures, the known results often do not apply directly to our situation and must be reformulated and reproved. In particular, in Propositions 3.4 and 3.6 (whose proofs constitute more than half of this section) we provide a way to calculate the values of invariants of a Legendrian knot in an overtwisted contact structure from its front on the torus.

Please note that all the knots considered in this section are *oriented*.

Definition 3.1. Let K be a Legendrian knot in a contact structure ζ .

(i) Assume K is homologous to zero. Denote by K' be the transverse knot obtained by small shift of K in the direction normal to the contact planes. The linking number

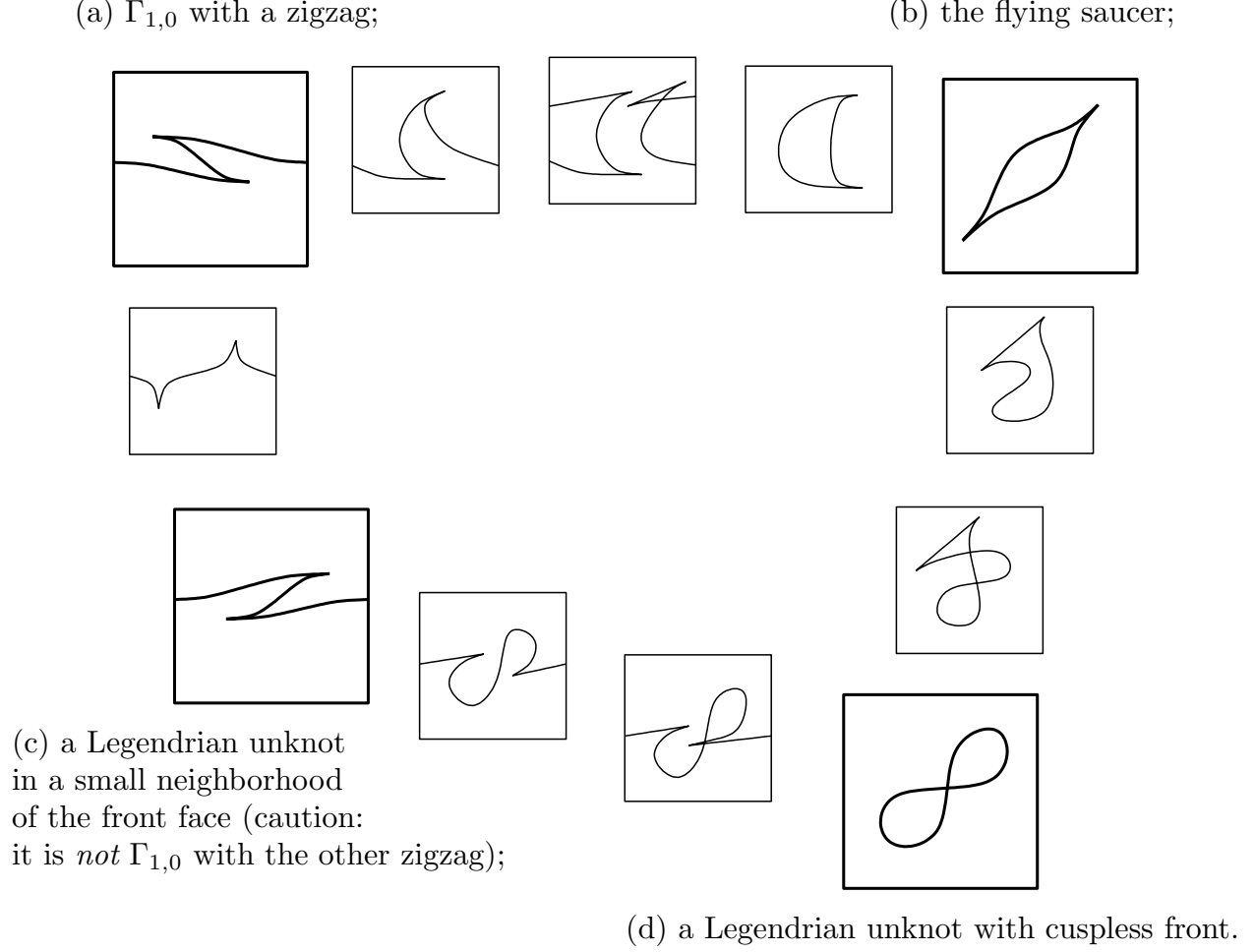


Figure 8: Four isotopic Legendrian unknots.

$lk(K, K')$ (i.e. the number of times, counted with signs, K' intersects a Seifert surface of K) is called the *Thurston-Bennequin invariant* of K and denoted by $tb(K)$. Note that $tb(K)$ is indeed determined by K alone.

(ii) Assume that ζ is parallelized. The index (number of revolutions) of the tangent vector to K with respect to the parallelization is called the *rotation* of the knot K and denoted by $rot(K)$.

The Thurston-Bennequin invariant is a particular case of the self-linking number of a (null-homologous) framed knot; two topologically isotopic Legendrian knots have equal Thurston-Bennequin invariants if and only if they are isotopic as framed knots. Sometimes (e.g. in [20]) the isotopy class of framed knots is used as a natural (though not so convenient) generalization of the Thurston-Bennequin invariant to homologically nontrivial knots. For a numerical version of this generalization (“affine self-linking number”) see [19].

The parallelization of the contact structure in Definition 3.1(ii) does not have to be neither unique nor defined on the whole manifold: rotations of all knots contained in a fixed subset of the manifold can be calculated with respect to one fixed parallelization. Note also that the rotation is actually an invariant of Legendrian *curves* rather than knots, as

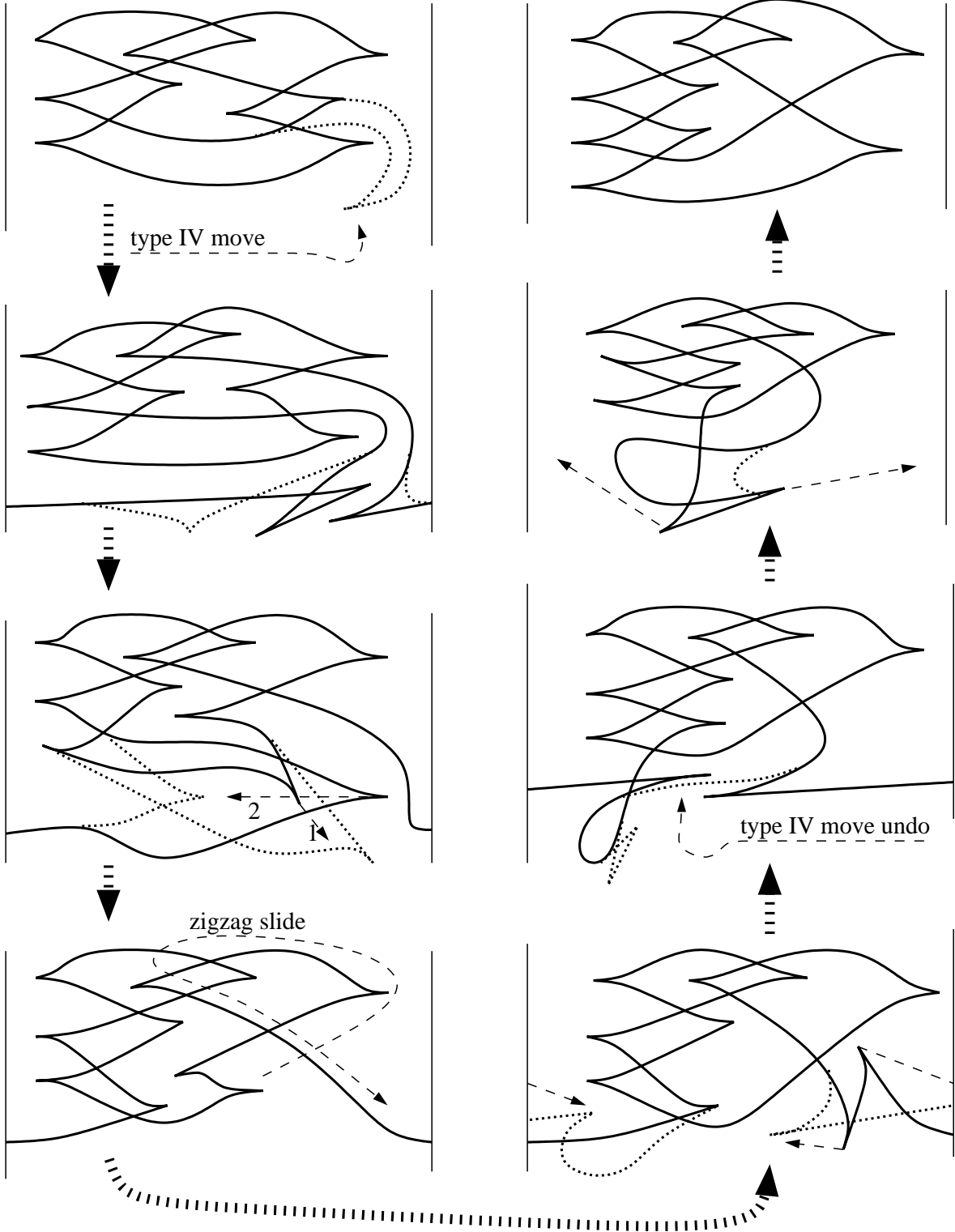


Figure 9: The Chekanov examples regarded as Legendrian knots in an overtwisted contact structure are isotopic.

it remains unchanged under a homotopy through Legendrian curves with possible self-intersections.

Furthermore, the rotation changes sign when the knot orientation is reversed. On the other hand, the Thurston-Bennequin invariant of a Legendrian knot does not depend on its orientation: reversing the orientation of K changes also the orientation of K' , so the linking number remains intact.

Equipped with those two invariants (in addition to the topological knot type, which is obviously also an invariant of Legendrian isotopy) we may ask a natural question: is this set of invariants complete?

Question 3.2. *Let \mathcal{L}_M be the set of Legendrian isotopy classes of knots in M , \mathcal{K}_M the set of topological knot types. Consider the map $\mathcal{T} : \mathcal{L}_M \rightarrow \mathcal{K}_M \times \mathbf{Z} \times \mathbf{Z}$ associating with a Legendrian knot K its topological type, rotation and Thurston-Bennequin invariant.*

- (a) *Is \mathcal{T} injective?*
- (b) *Is \mathcal{T} surjective?*

In general, the answer to both parts is “no”.

- (a) There are known examples of topologically isotopic Legendrian knots (including some in the standard tight contact structure on \mathbf{R}^3) which have equal invariants but are not Legendrian isotopic ([3], [11], [16]; the pair of knots from Example 2.6 has this property as well). In Section 4 we discuss this question for overtwisted contact structures.
- (b) It is known that in the standard tight contact structure on \mathbf{R}^3 the values of invariants of any Legendrian knot K are related via the congruence $tb(K) + rot(K) \equiv 1 \pmod{2}$. Lemma 4.6 allows to generalize this result to homotopically trivial Legendrian knots in an arbitrary contact manifold.

Moreover, in several contact manifolds there are various restrictions on the range of the values of invariants, the best known⁷ being the Bennequin inequality [2].

Theorem 3.3 (Bennequin inequality). *For K a Legendrian knot in the standard tight contact structure we have*

$$tb(K) + rot(K) \leq -\chi(K),$$

where $\chi(K)$ is the maximal Euler characteristic of a Seifert surface of K .

Fuchs and Tabachnikov in [12] provide a way of reading the values of rot and tb from the diagram data. We give an analogous result for (S^3, ζ_1) , but first we need to introduce some notation.

Consider the homotopy type of a front on the torus as a curve in T^2 , i.e. an element $(\alpha, \beta) \in \pi_1 T^2 \simeq \mathbf{Z}^2$. We choose the generators so that $(1, 0)$ is the horizontal line oriented left-to-right, and $(0, 1)$ —the vertical line oriented upwards. We will denote the homotopy type of the diagram of K by $(\alpha(K), \beta(K))$.

In a front diagram in the standard tight contact structure there are two sorts of (unoriented) cusps: those pointing to the left and those pointing to the right; and each

⁷ Other similar in spirit bounds have been found by Fuchs and Tabachnikov in [12].

of them may be passed either upward or downward. Also, the branches (pieces between cusps) of an oriented front are either traversed left-to-right or right-to-left (and these two types alternate).

The same can be said about the fronts on the torus, with proper understanding of “up”, “down”, “left” and “right”. Pick the coorientation of ξ pointing up near the front face. It induces a normal vector field ν along the knot diagram. A cusp is *left* if it points to the left after rotating so that ν is directed upwards, and *right* otherwise. The same convention applies to the orientation of branches. A cusp (left or right) is *ascending* if it is traversed in the direction of ν and *descending* otherwise. Figure 10 shows all kinds of cusps.

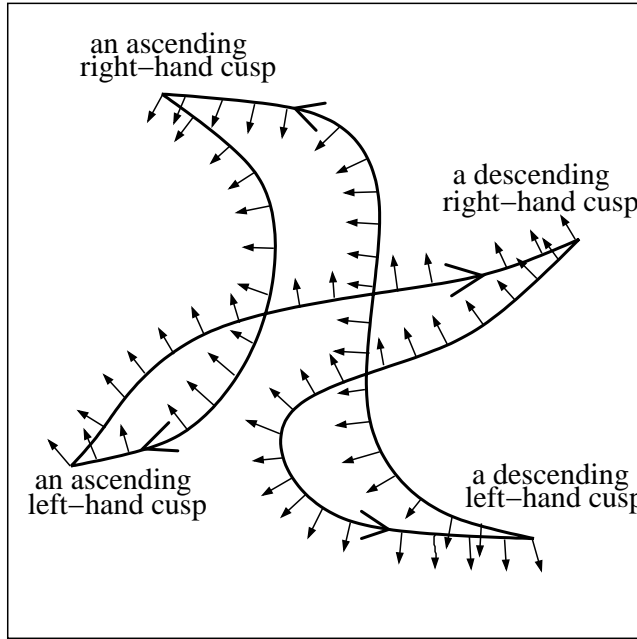


Figure 10: Types of cusps.

Proposition 3.4. *Consider a Legendrian knot $K \subset (S^3, \xi)$ whose diagram $\pi(K)$ has the homotopy type $(\alpha(K), \beta(K))$ and contains $cusp_+(K)$ positive cusps and $cusp_-(K)$ negative ones. Then*

$$rot(K) = \frac{1}{2}(cusp_+(K) - cusp_-(K)) - \alpha(K) - \beta(K).$$

Proof: We need to pick a convenient parallelization of ξ . A nice candidate would be a vector field which is constant in the xyz coordinates of Construction 1.8, say, pointing in the positive direction of the x axis (let us call this vector field \mathcal{X}). Unfortunately, \mathcal{X} does not induce a vector field on the sphere. We can, however, find a parallelization of ξ on S^3 whose pull-back to the cube coincides with \mathcal{X} in a region $\mathcal{C}_0 \supset [\varepsilon, 1 - \varepsilon]^3$. We may assume

that the knot lies entirely in \mathcal{C}_0 except for a finite number of small segments at the points of intersection with the side faces.

Now we calculate the number of revolutions made by the tangent vector κ within the region \mathcal{C}_0 . Observe that κ coincides with \mathcal{X} at each left positive cusp and each right negative cusp, and that at the left positive cusps it is locally turning in the positive direction and at the right negative ones—in the negative direction. Therefore, the contribution to $rot(K)$ from the parts of K contained in \mathcal{C}_0 is $cusp_+^{left}(K) - cusp_-^{right}(K)$. Since K must have exactly as many left cusps as right ones, $cusp_+^{left}(K) - cusp_-^{right}(K) = \frac{1}{2}(cusp_+(K) - cusp_-(K))$.

Finally, we have to account for the contribution to $rot(K)$ of the segments at the intersection with the side faces. Considering a small loop around the image of the front (resp. back) face it is easy to see that, since the parallelization extends to S^3 , the tangent vector necessarily makes one turn (see 3). When we traverse the loop in the direction of the chosen generator, the turn is taken in the negative direction. A continuity argument shows that the same is true for any Legendrian knot crossing the side face. Counting with signs, K intersects the side faces $\alpha(K) + \beta(K)$ times. Hence the formula. \square

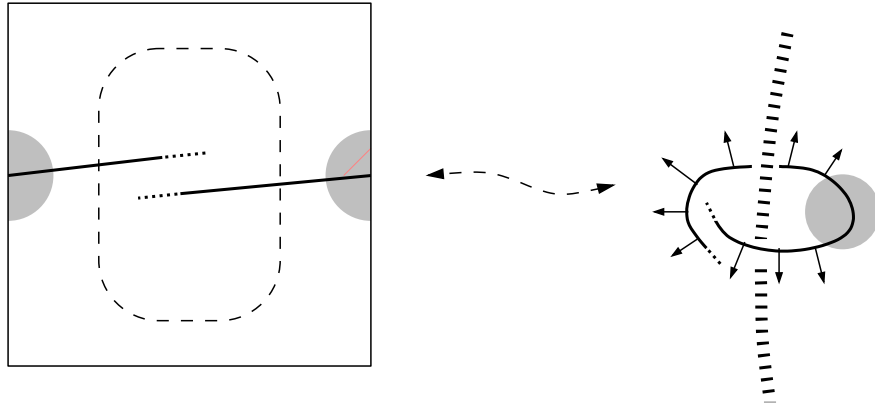


Figure 11: Crossing the side face contributes to rotation.

In order to formulate the results concerning the Thurston-Bennequin invariant, we need to distinguish between positive and negative crossings. We adopt the usual convention, recalled in Figure 12. However, the front diagrams of Legendrian knots traditionally do not show the over/under crossing indication (since it is redundant), which makes reading the sign of a crossing somewhat inconvenient.



Figure 12: Positive and negative crossings.

In the standard tight contact structure, a helpful observation is that crossings between a branch oriented left-to-right and one oriented right-to-left is always negative, while a crossing between two branches of matching orientations is positive. The same (with “left” and “right” understood as explained above) is true for the contact structure ξ and fronts on the torus, provided that the x coordinates of the two branches differ by less than π ; if they differ by more than π , the situation is opposite.

The following lemma temporarily leaves the realm of contact topology. For K an arbitrary topological knot in $S^3 \setminus (c_f \cup c_b)$ we may still consider its diagram (projection) on the torus. There will be no cusps anymore (not for a knot in general position), but the homotopy type $(\alpha(K), \beta(K))$, as well as the distinction between positive and negative crossings, still make sense.

Lemma 3.5. *Suppose that*

- (i) K_1 and K_2 are topological knots in $S^3 \setminus (c_f \cup c_b)$;
- (ii) the diagram $\pi(K_i)$ has the homotopy type $(\alpha(K_i), \beta(K_i))$;
- (iii) there are $cross_+(K_1, K_2)$ positive crossings and $cross_-(K_1, K_2)$ negative ones with one strand from K_1 and the other from K_2 .

Then the linking number (in the sphere) is given by the formula

$$lk(K_1, K_2) = \frac{1}{2} (cross_+(K_1, K_2) - cross_-(K_1, K_2) - \alpha(K_1)\beta(K_2) - \alpha(K_2)\beta(K_1))$$

Proof: The formula $lk(K, L) = \frac{1}{2} (cross_+(K_1, K_2) - cross_-(K_1, K_2))$ holds for knots in \mathbf{R}^3 and their diagrams on the plane. We can consider a knot in the 3-sphere as a knot in $\mathbf{R}^3 = S^3 \setminus \{*\}$. To get its diagram on the plane from the one on the torus it is enough to close up the loose ends which arise when we cut the torus and unfold it to a square (see Figure 13). Notice that all the lines connecting the horizontal loose ends overcross those attached to the vertical ends. Hence the additional lines contribute $\alpha(K_1)\beta(K_2) + \alpha(K_2)\beta(K_1)$ crossings counted with signs.

The formula follows. □

Proposition 3.6. *Let K be a Legendrian knot in (S^3, ξ) whose diagram has the homotopy type $(\alpha(K), \beta(K))$, contains $cusp(K)$ cusps, $cross_+(K)$ positive crossings and $cross_-(K)$ negative crossings. Then*

$$tb(K) = cross_+(K) - cross_-(K) - \frac{1}{2} cusp(K) - \alpha(K)\beta(K)$$

Proof: By Definition 3.1(i) and Lemma 3.5, $tb(K) = lk(K, K') = \frac{1}{2} (cross_+(K, K') - cross_-(K, K') - \alpha(K)\beta(K') - \alpha(K')\beta(K))$, where K' is the knot obtained from K by pushing it slightly in the direction of the coorientation of ξ . The diagram (front on the torus) of K' is also obtained by a small shift from that of K . Therefore

- each positive crossing in the diagram of K gives rise to two positive crossings between the diagrams of K and K' ;

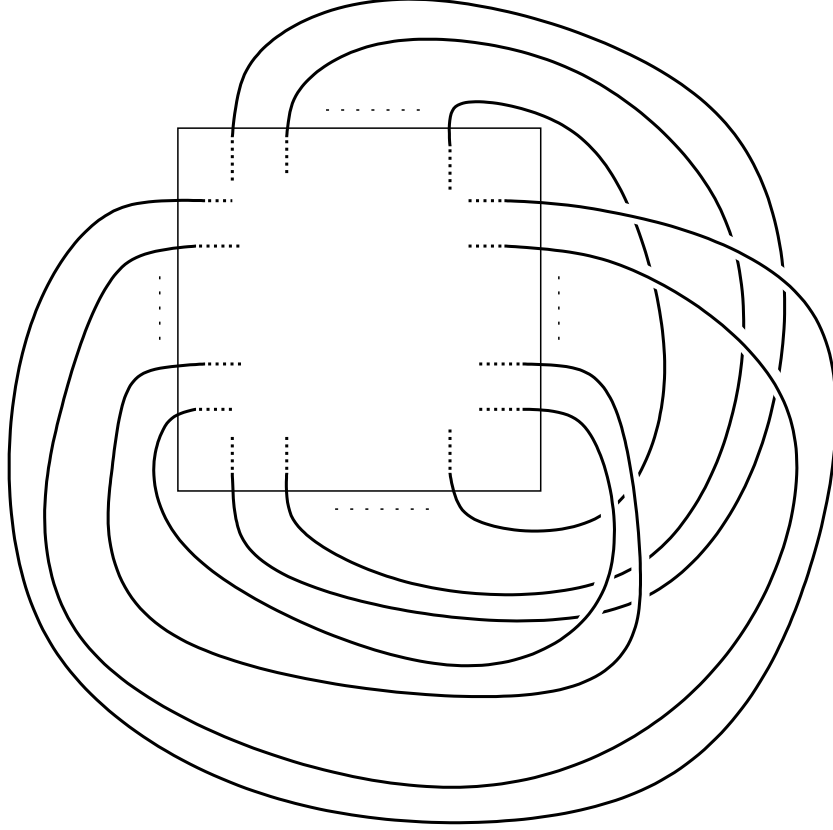


Figure 13: Closing up the diagram.

- each negative crossing in the diagram of K gives rise to two negative crossings;
 - each cusp in the diagram of K gives rise to a negative crossing;
- and these are all the crossings between the diagrams of K and K' .

Certainly, $\alpha(K') = \alpha(K)$ and $\beta(K') = \beta(K)$.

Thus,

$$\begin{aligned} lk(K, K') &= \frac{1}{2} (cross_+(K, K') - cross_-(K, K') - \alpha(K)\beta(K') - \alpha(K')\beta(K)) = \\ &= \frac{1}{2} (2 cross_+(K) - 2 cross_-(K) - cusp(K) - 2\alpha(K)\beta(K)). \end{aligned}$$

The formula follows. □

Propositions 3.4 and 3.6 imply that the values of invariants are always uniquely determined by the diagram of a Legendrian knot, even if the knot itself is not. (This is the case, for example, with some of the knots $\Gamma_{m,n}$ defined in Example 2.3.) We want to calculate rot and tb of $\Gamma_{m,n}$'s; to this end it is necessary to choose an orientation for each of them. We do it in an obvious way, requiring that $\alpha(\Gamma_{m,n}) = m$ and $\beta(\Gamma_{m,n}) = n$. Thus, $\Gamma_{-m,-n} = \bar{\Gamma}_{m,n}$ (i.e. $\Gamma_{m,n}$ with the opposite orientation).

Example 3.7. With the orientation as described above, we have $rot(\Gamma_{m,n}) = -m - n$ and $tb(\Gamma_{m,n}) = -mn$.

Note that topologically any $\Gamma_{m,n}$ is a torus knot of type (m,n) ; in particular, for $|m| = 1$ (or $|n| = 1$) it is an unknot. Therefore for each integer n we get a Legendrian unknot $\Gamma_{1,n}$ of rotation number $-n - 1$ and Thurston-Bennequin invariant $-n$.

4 The Classification Theorem

In this section we formulate and prove the theorem announced in the introduction as a generalization (with completely different methods of proof) of the main theorem of [4].

Theorem 4.1. *Let ξ be an overtwisted contact structure on a 3-manifold M , Δ an overtwisted disk in (M, ξ) , K and L Legendrian knots in $M \setminus \Delta$. Assume that ξ is trivializable as a plane bundle. Let \mathcal{K} be the topological knot type of K . Assume that:*

- (a) *there are infinitely many non-isotopic framed knots in \mathcal{K} ;*
- (b) *K and L are isotopic as framed knots (with Legendrian framing); and*
- (c) *$\text{rot}(K) = \text{rot}(L)$, where rot is calculated with respect to some parallelization of ξ .*

Then K and L are Legendrian isotopic.

Remark 4.2. The assumption (a) is satisfied for all knots in a manifold M (not necessarily closed) which is not realizable as a connected sum $M' \# (S^1 \times S^2)$ (see Theorem 2.0.5 in [19]).

For homologically trivial knots the assumption (b) is equivalent to the conjunction of the following two conditions:

- (b1) K and L are isotopic as topological knots, and
- (b2) $tb(K) = tb(L)$.

The proof of this theorem relies on two lemmas. Lemma 4.7 explains the role of the overtwisted disks. Lemma 4.6 generalizes (to an arbitrary contact structure) Theorem 4.4 of [12]; its main ingredient is the notion of adding a zigzag, a.k.a. stabilization, also introduced by Fuchs and Tabachnikov in [12]. They understand adding a zigzag as a special case of the operation of connected summation of Legendrian knots. For us, this approach would have serious disadvantages: the connected sum of Legendrian knots in an arbitrary contact structure is not always well defined. We will, therefore, content ourselves with a naïve diagrammatic definition of adding a zigzag.⁸

Definition 4.3. Let (M, ζ) be a contact manifold, K a Legendrian knot in it. Pick a point $x_0 \in K$; there is a neighborhood $V \ni x_0$ such that $\zeta|_V$ is the standard contact structure on \mathbf{R}^{39} (and $K \cap V$ a long Legendrian knot in it), thus it makes sense to talk about the front diagram of $K \cap V$. Now replace a small cusplless segment of $K \cap V$ with

⁸ There is another fairly general notion which contains adding a zigzag as a special case, namely the (Legendrian) satellite construction (see [17]).

⁹ A *Darboux chart* in the nomenclature of [20].

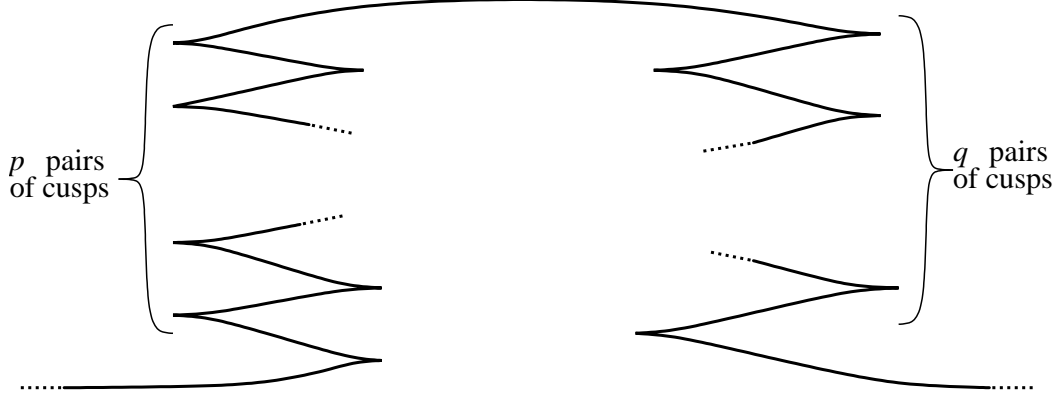


Figure 14: Adding a zigzag.

one containing p pairs of ascending cusps and q pairs of descending cusps (see Figure 14). We call the resulting knot *the p, q -stabilization of K* and denote it by $Z_{p,q}(K)$.

Example 4.4. Figure 15 shows a few of the Legendrian knots obtained by adding zigzags to the standard “flying saucer” Legendrian unknot (depicted in Figure 8(b)). We will not distinguish between the operation of adding a zigzag and the result of this operation applied to the standard unknot, denoting these knots simply by $Z_{p,q}$.

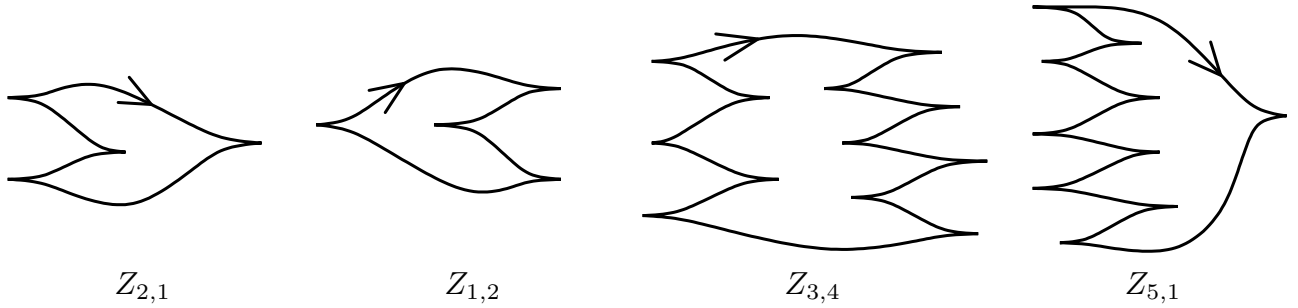


Figure 15: Examples of zigzags.

One needs to show that $Z_{p,q}(K)$ is well defined and does not depend on the choice of the point x_0 where the new cusps are placed. The classical argument, based on sliding pair of cusps along the knot (cf. [12], Lemma 4.3 with Figures 17 and 18, which are recalled here as Figure 16), applies directly.

The following proposition collects a couple of (obvious, but useful) facts about adding zigzags.

Proposition 4.5.

- (a) $Z_{p,q}(Z_{p',q'}(K))$ is Legendrian isotopic to $Z_{p+p',q+q'}(K)$;
- (b) $\text{rot}(Z_{p,q}(K)) = \text{rot}(K) + p - q$; and
- (c) the Legendrian framing of $Z_{p,q}K$ is the Legendrian framing of K with $p + q$ negative twists added (for zero-homologous K this means $\text{tb}(Z_{p,q}(K)) = \text{tb}(K) - p - q$.)



Figure 16: Sliding pair of cusps (elementary zigzags).

□

Lemma 4.6. *If K and L are two (long or short) Legendrian knots in an arbitrary contact manifold (M, ζ) which are topologically isotopic, then there exist two Legendrian knots $K_Z = Z_{p,q}(K)$ and $L_Z = Z_{p',q'}(L)$ such that K_Z is Legendrian isotopic to L_Z .*

Proof: We begin by choosing a topological isotopy between K and L which makes changes piece by piece only. Namely, for $\{K_t, t \in [0, 1]\}$, $K_0 = K$, $K_1 = L$, we assume that there are finitely many points $t_0 = 0 < t_1 < t_2 < \dots < t_n = 1$ and balls $B_1, B_2, \dots, B_n \subset M$ such that

- $\zeta|_{B_i}$ is the standard tight contact structure on \mathbf{R}^3 ;
- for $t_{i-1} \leq t \leq t_i$, K_t is constant outside B_i .

Now it is enough to study the isotopies $\{K_t|_{B_i}, t \in [t_{i-1}, t_i]\}$ as isotopies of Legendrian knots in the standard tight contact structure on \mathbf{R}^3 . By Theorem 4.4 of [12], $Z_{p_{i-1}, q_{i-1}}(K_{t_{i-1}})$ is Legendrian isotopic to $Z_{p_i, q_i}(K_{t_i} \# Z_{p_i, q_i})$ for some $p_{i-1}, q_{i-1}, p_i, q_i$. An easy inductive argument ends the proof. □

Lemma 4.7 (creating zigzags). *Let $V(\Delta)$ be a small neighborhood of an overtwisted disk Δ in M , L a Legendrian knot in $M \setminus \Delta$. Assume that (under the identification of $V(\Delta)$ with a subset of (S^3, ζ_1) described above) the projection of the curve $\ell = L \cap V(\Delta)$ onto the torus is a straight line segment (as in the top part of Figure 18, where the shaded area symbolizes $V(\Delta)$).¹⁰ Then for any p and q there is a Legendrian knot $\ell_{p,q}$ in U coinciding with ℓ outside a compact set and such that $Z_{p,q}(K \setminus \ell) \cup \ell_{p,q}$ is Legendrian isotopic to K .*

¹⁰ Note that, even though the front on the torus of the top left part of Figure 18 corresponds to two different Legendrian curves, the condition that L is in $M \setminus \Delta$ actually excludes one of them.

Proof: We begin by checking this statement for elementary zigzags. Figure 18 shows an isotopy between L and a Legendrian knot coinciding outside $V(\Delta)$ with $Z_{0,1}(L)$ or $Z_{0,1}(L)$, depending on the orientation of ℓ .

In order to produce the other elementary zigzag, first perform the type I Reidemeister move on ℓ , so that it crosses some smaller neighborhood of Δ three times: twice in the same direction as before and once (between cusps) in the opposite direction. By a small isotopy we can ensure that the slope of the segment between cusps is the smallest, see Figure 17. Then the corresponding segment of the curve lies closest to the disk: we can replace $V(\Delta)$ with a smaller neighborhood $V'(\Delta)$ which contains only the segment going in the opposite direction to that of the original ℓ .

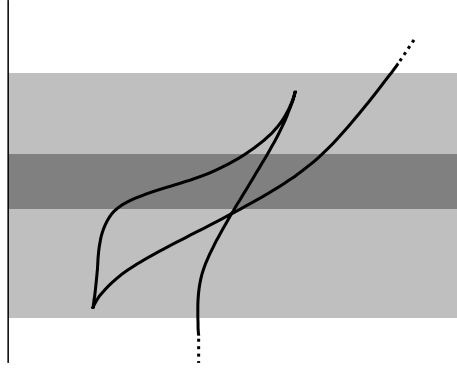


Figure 17: Changing the direction of ℓ

In order to prove the lemma for an arbitrary zigzag $Z_{p,q}$, use $p + q$ disjoint slices of $V(\Delta)$ (neighborhoods of $p + q$ parallel copies of Δ), to produce p copies of $Z_{1,0}$ and q copies of $Z_{0,1}$. Then slide the newly created zigzags along the knot until they leave the whole $V(\Delta)$. \square

Proof of Theorem 4.1: There is a Legendrian isotopy moving K in $M \setminus \Delta$ so that it coincides with L along a small segment, which we will call ℓ . By assumption, there is a topological isotopy between K and L ; without loss of generality we may assume that the isotopy is constant on ℓ .

Pick a neighborhood V containing Δ and such that $\overline{V} \cap (K \cup L) = \ell$. By Lemma 4.6, $K \setminus \ell$ and $L \setminus \ell$ (considered as *long* Legendrian knots in $M \setminus V$) are Legendrian isotopic modulo adding zigzags, i.e. $Z_{p_K, q_K}(K \setminus \ell)$ and $Z_{p_L, q_L}(L \setminus \ell)$ are Legendrian isotopic, thus also $Z_{p_K, q_K}K \simeq Z_{p_L, q_L}L$ as Legendrian knots in M .

By Proposition 4.5(b) we have then $\text{rot}(K) + p_K - q_K = \text{rot}(L) + p_L - q_L$. By assumption 4.1(c) $\text{rot}(K) = \text{rot}(L)$, thus

$$p_K - q_K = p_L - q_L \quad (*)$$

.

Adding a p, q -zigzag introduces $p + q$ extra negative twists to the Legendrian framing.

The Legendrian isotopy between $Z_{p_K, q_K}K$ and $Z_{p_L, q_L}L$ induces an isotopy of framed knots. Since Legendrian framings of K and L also coincide (see 4.1b), we see that the

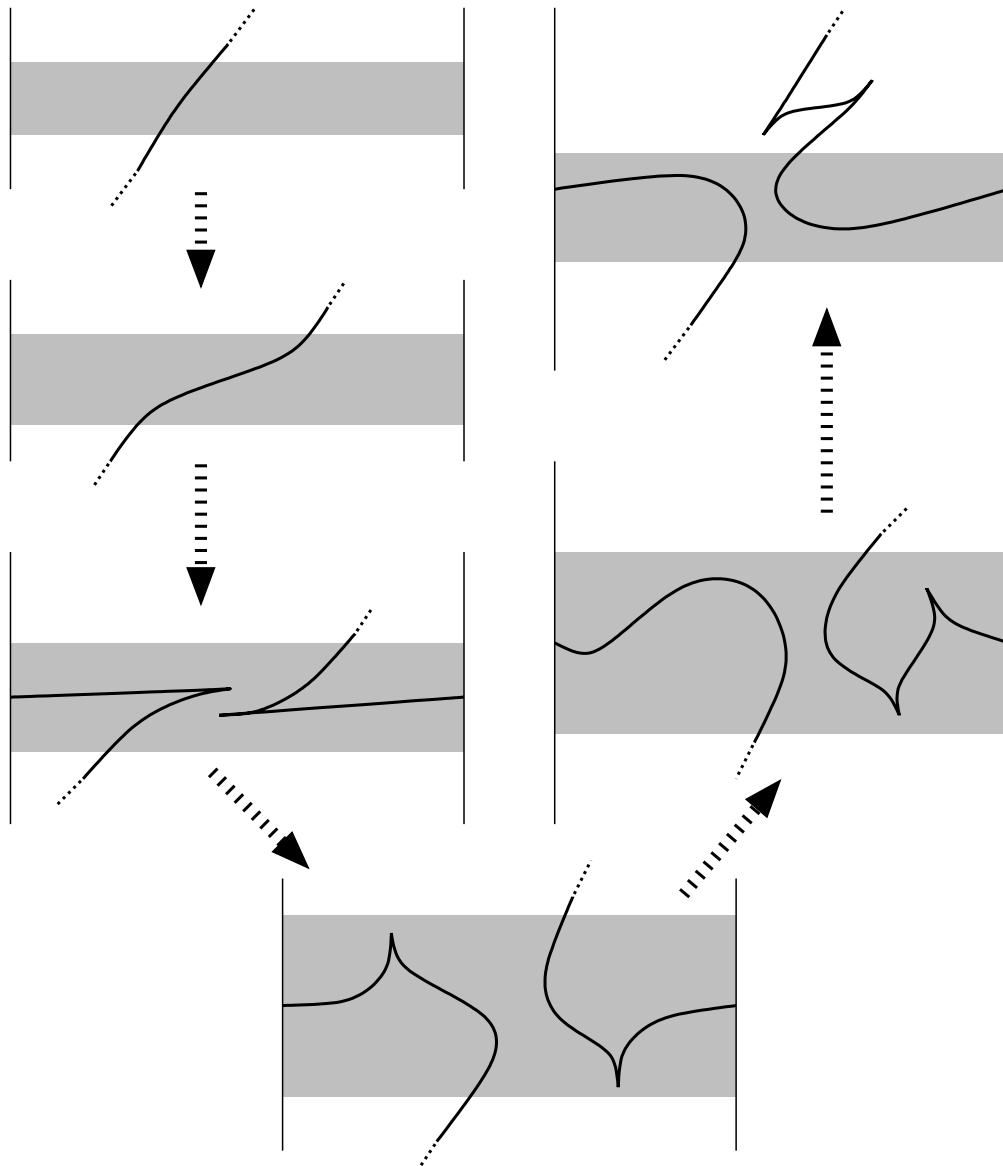


Figure 18: Making a zigzag (out of nothing).

effect of adding $p_K + q_K$ negative twists to the Legendrian framing of K must be the same as that of adding $p_L + q_L$ ones. This implies that

$$p_K + q_K = p_L + q_L, \quad (**)$$

provided that the condition 4.1(a) is satisfied.

From (*) and (**) it follows that $p_K = p_L$ and $q_K = q_L$; for simplicity, we will denote these numbers by p and q respectively.

By Lemma 4.7, $K \simeq Z_{p,q}(K \setminus \ell) \cup \ell_{p,q}$ and $L \simeq Z_{p,q}(L \setminus \ell) \cup \ell_{p,q}$; but we have also $Z_{p,q}(K \setminus \ell) \simeq Z_{p,q}(L \setminus \ell)$. This proves $K \simeq L$. \square

Definition 4.8. A Legendrian knot is called *loose* if its complement is overtwisted.

For example, all standard knots (as defined at the end of Section 2) are necessarily loose; also any knot whose front on the torus does not cross a fixed meridian of the torus (as on Figure 3) is loose.

On the other hand, in [4] the author proved that the knot $\Gamma_{-1,1}$ is non-loose. It have been believed a sort of one-time phenomenon (even the name originally proposed by Eliashberg and Fraser in [6] was “exceptional knots”). Etnyre and Ng conjecture that $\Gamma_{-1,1}$ (is isotopic to $\Gamma_{-1,1}$ and) is the only non-loose Legendrian unknot that can be found in any overtwisted contact structure on S^3 (Conjectures 41 and 42 in [10]). This is not true; in Proposition 5.5 we prove that all the knots $\Gamma_{m,n}$ for which $mn < 0$ are non-loose. In particular, $\Gamma_{-1,n}$ (for $n = 1, 2, 3 \dots$) are all different (distinguishable by *rot* and *tb*) non-loose Legendrian unknots.

The above Lemma 4.7 (thus also Theorem 4.1) deals with loose Legendrian knots only. This assumption is, of course, essential: two topologically isotopic Legendrian knots with the same values of rotation and Thurston-Bennequin invariant may be Legendrian non-isotopic simply because one of them is loose while the other is not (cf. Example 5.7). But even for two loose knots Theorem 4.1 is not necessarily applicable. Namely, there exist two loose Legendrian knots for which there is no overtwisted disk disjoint with *both* of them.

Proposition 4.9. *Every overtwisted disk in (S^3, ζ_1) intersects either $\Gamma_{0,1}$ or $\Gamma_{1,0}$.*

Proof: We want to show that the open manifold $M = S^3 \setminus (\Gamma_{0,1} \cup \Gamma_{1,0})$ is tight; it is enough to prove tightness of its universal cover \widetilde{M} (because a hypothetical overtwisted disk in M would lift to \widetilde{M}). The idea of this proof is the same as employed in [4] in the proof of Lemma 4.2.1: we will find a contactomorphism of \widetilde{M} with an open subset of \mathbf{R}^3 with the tight contact structure $\zeta' = \ker(\cos x \, dz - \sin x \, dy)$ described in Example 1.2 (a subset of a tight manifold is, of course, also tight).

Step 1: Topological description

We will see M as made of three parts: two solid tori $M_f = M \cap \text{pr}_{\mathcal{C}}([0, 1/3] \times [0, 1]^2)$ and $M_b = M \cap \text{pr}_{\mathcal{C}}([2/3, 1] \times [0, 1]^2)$, and the “middle slice” $M_m = M \cap \text{pr}_{\mathcal{C}}([1/3, 2/3] \times [0, 1]^2)$, glued together along two annuli: $A_0 = M_f \cap M_m$ and $A_1 = M_b \cap M_m$. The middle slice is diffeomorphic to $T^2 \times [0, 1]$ with a meridian removed from one component of the boundary and a latitude—from the other; hence its universal cover $\widetilde{M}_m = \mathbf{R}^2 \times [0, 1] \setminus L$, where L consists of two infinite families of parallel lines, one in the universal cover of each boundary component of $T^2 \times [0, 1]$. In \widetilde{M}_m the annulus A_0 (resp. A_1) lifts to the union of infinitely many stripes. Along each stripe we need to attach a copy of \widetilde{M}_f (resp. \widetilde{M}_b), which is diffeomorphic to $H \times \mathbf{R}$ for H a half-disk.¹¹ Thus, we get the space pictured in Figure 19.

Step 2: Contact structure

First, notice that \widetilde{M}_m can be contact embedded into (\mathbf{R}^3, ζ') so that its image consists of the slice $\{0 \leq x \leq \pi/2\}$ with the subset L (equal to $\{x = 0, y \in \mathbf{Z}\} \cup \{x = \pi/2, z \in \mathbf{Z}\}$) removed.

¹¹ From the description of M we see that H is D^2 with a boundary point removed; we choose to see it as a half-disk to make the gluing picture easier to understand.

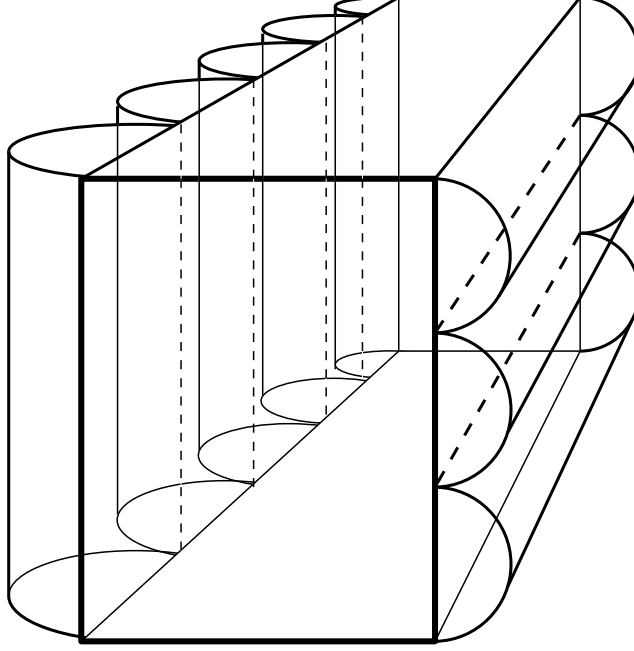


Figure 19: The universal cover \widetilde{M} .

Now we need to recall the construction used in the proof of Lemma 4.2.1 in [4]. We considered the universal cover of $S^3 \setminus \Gamma_{-1,1}$ (with the same contact structure ζ_1), which again could be described as the union $\widetilde{M}_0 \cup \widetilde{M}_1$, with $M_0 = (S^3 \setminus \Gamma_{-1,1}) \cap \text{pr}_C([0, 1/2] \times [0, 1]^2)$ and $M_1 = (S^3 \setminus \Gamma_{-1,1}) \cap \text{pr}_C([1/2, 1] \times [0, 1]^2)$, glued together along an annulus A . Then, we constructed a contact embedding $J : \widetilde{M} \hookrightarrow (\mathbf{R}^3, \zeta)$ (where ζ is the contact structure defined in Example 1.1), starting by setting its values on \widetilde{A} so that $J(\widetilde{A}) = \{x = 0\}$. Thus \widetilde{M}_0 maps into the half-space $\{x \geq 0\}$.

Since the spaces \widetilde{M}_f and \widetilde{M}_b are both contactomorphic to \widetilde{M}_0 , we have contact embeddings $j_f : (\widetilde{M}_f, \zeta_1) \rightarrow (\mathbf{R}^3, \zeta)$ and $j_b : (\widetilde{M}_b, \zeta_1) \rightarrow (\mathbf{R}^3, \zeta)$. This is not exactly what we want:

- the contact structure on the target \mathbf{R}^3 should be ζ' rather than ζ ;¹² and
- the boundary of \widetilde{M}_f (resp. \widetilde{M}_b) should not be mapped onto the whole plane, but onto a single stripe.

To get rid of both problems at once it is enough to notice that each of the subsets $U_n = (\pi/2, 0] \times (n, n+1) \times \mathbf{R}$ and $V_n = [\pi/2, \pi) \times \mathbf{R} \times (n, n+1)$ in (\mathbf{R}^3, ζ'_0) is contactomorphic to the half-space $\{x \geq 0\}$ in (\mathbf{R}^3, ζ) (and the contactomorphism, of course, maps the boundary of U_n and V_n onto the plane $\{x = 0\}$).

Thus we get an embedding of a copy of \widetilde{M}_f into each U_n and a copy of \widetilde{M}_b into each V_n . The union of boundaries $\bigcup_n \partial U_n \cup \bigcup_n \partial V_n$ coincides with the boundary of the image

¹² Those two are, of course, isomorphic; but since we are in the process of constructing a specific embedding, we need proceed with greater exactness than just up to a contactomorphism.

of \widetilde{M}_m via its previously constructed embedding into $\{0 \leq x \leq \pi/2\} \subset (\mathbf{R}^3, \zeta'_0)$. The flexibility which we enjoy when we start to construct the maps j_f and j_b is sufficient to ensure that the embedding of \widetilde{M}_m and those of (the infinitely many copies of) \widetilde{M}_f and \widetilde{M}_b form together a contact embedding $(\widetilde{M}, \zeta_1) \hookrightarrow (\mathbf{R}^3, \zeta'_0)$. \square

Thus we have left unanswered the following question.

Question 4.10. Are $\Gamma_{0,1}$ and $\Gamma_{1,0}$ Legendrian isotopic?

From Theorem 4.1 alone we can draw no conclusion in this matter; in fact, the answer is unknown to the author.

5 The Catalog of Legendrian Knots

Let ξ be an overtwisted contact structure on S^3 . In this section we concentrate on existence results for Legendrian knots in ξ . Our goal is to give the answer (as comprehensive as possible) to Question 3.2(b), using the results of Sections 2 and 4.

Theorem 5.1. *For any topological knot type \mathcal{K} and any pair of integers r and t such that $r + t \equiv 1 \pmod{2}$, there is a Legendrian knot L in (S^3, ξ) realizing \mathcal{K} with $\text{rot}(L) = r$ and $\text{tb}(L) = tb$.*

Lemma 5.2. *For any pair of integers r and t such that $r + t \equiv 1 \pmod{2}$ there is a Legendrian unknot $U = U(r, t)$ in ξ with $\text{rot}(U) = r$ and $\text{tb}(U) = tb$.*

Proof: We will draw front diagrams of the desired unknots. Their appearance depends on the actual values of r and t as follows:

- (a) For the zigzag $Z_{p,q}$ (see Figure 15) we have $\text{rot}(Z_{p,q}) = p - q$ and $\text{tb}(Z_{p,q}) = -p - q - 1$ (with the orientation so chosen that there is $2p + 1$ ascending and $2q + 1$ descending cusps); the pairs of integers (r, t) that can be obtained this way are all those satisfying Bennequin inequality for unknots, i.e. $t < 0$ and $|r| \leq |t|$.
- (b) The rotation of the knot whose front diagram on the cylinder can be seen in the left part of Figure 20 is equal to $p - q$ and its Thurston-Bennequin invariant is $p + q - 1$; therefore such knots realize all pairs (r, t) with $t \geq 0$ and $|r| \leq |t|$;
- (c) Finally, the knot whose front diagram is depicted in the right part of Figure 20 has the Thurston-Bennequin invariant equal to $p - q$, while its rotation may be $p + q$ or $-p - q$, depending on the orientation; such knots exhaust all the remaining pairs (r, t) , i.e. those where $|r| \geq |t|$.

Proof of Theorem 5.1:

First, fix an overtwisted disk with its neighborhood $V(\Delta)$ and choose a Legendrian knot L_0 realizing the topological knot type \mathcal{K} so that the front diagram of its intersection with $V(\Delta)$ is a smooth arc as in the left part of Figure 21 (the curve labeled L_0). This is easily done, since any curve can be C_0 -approximated by a Legendrian one.

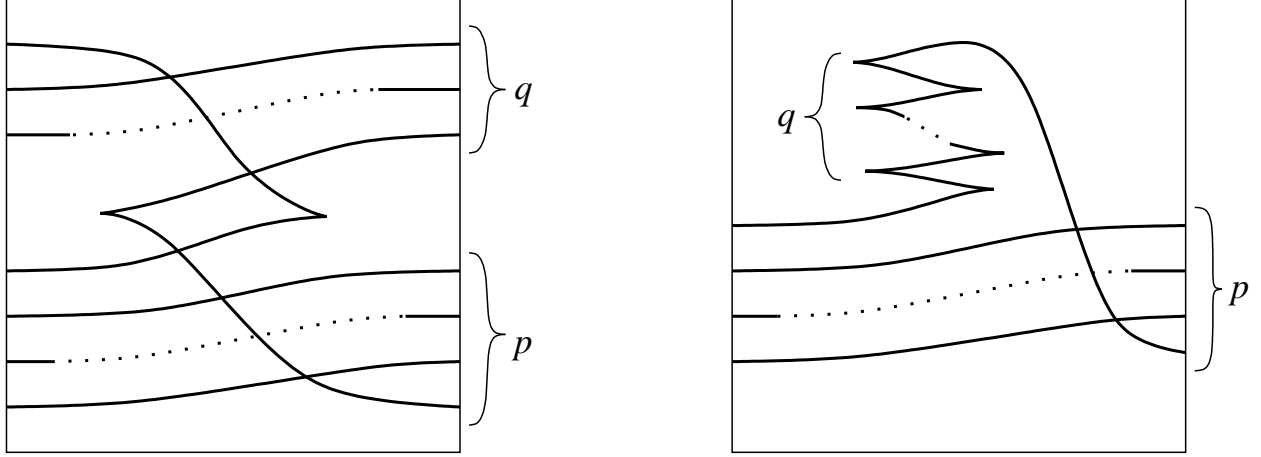


Figure 20: Legendrian unknots with $rot = 0$ and $tb = t \geq 0$.

Next, take a Legendrian unknot U with $rot(U) = r - rot(L_0)$ and $tb(U) = t - tb(L_0) - 1$, as constructed in the proof of Lemma 5.2. We may assume that U is contained in a smaller neighborhood of the overtwisted disk $V'(\Delta) \subset V(\Delta)$.

Then join $L_0 \cap V(\Delta)$ with the lowest strand of U in the way depicted in Figure 21 (in the case orientations do not match, first perform the dovetail move on one of the curves). We will denote the resulting knot by L .

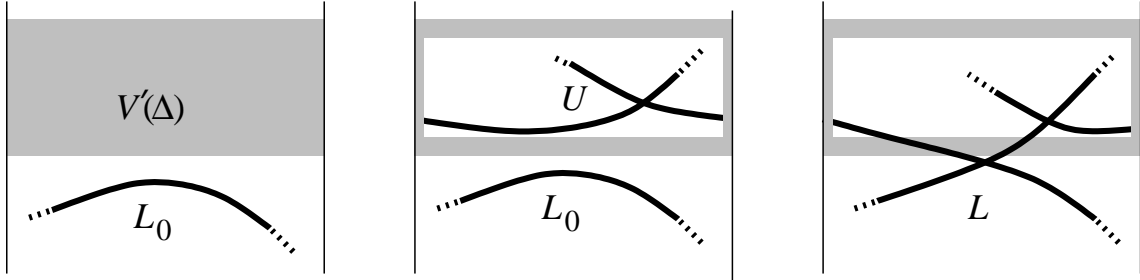


Figure 21: Constructing a Legendrian knot with pre-set invariants.

The operation defined above resembles the diagrammatic definition of the connected summation of Legendrian knots given by Etnyre and Honda in [9]. The reason why we do not introduce it as such is that the connected sum of Legendrian knots may not be well-defined in general setting. It retains, however, the following properties of the connected summation (cf. [9], Lemma 3.3; note that it is proved without using the fact that the result of the connected summation is independent of the choice of the point where the operation is performed):

- (i) the topological knot type of L is still \mathcal{K} , because L is the *topological* connected sum of L_0 with the unknot;
- (ii) $rot(L) = rot(L_0) + rot(U) = r$; and
- (ii) $tb(L) = tb(L_0) + tb(U) + 1 = t$.

Therefore L satisfies all the conditions we require. □

All the Legendrian knots constructed in the proof of Theorem 5.1 are loose. We can, however, formulate some classification results specifically for non-loose knots. Propositions 5.3 and 5.4 are corollaries of the Bennequin inequality. The first one of them has been pointed out to the author by Jacek Świątkowski.

Proposition 5.3. *Let ξ be an overtwisted contact structure on a manifold M , K a non-loose Legendrian knot in ξ . Then $-|tb(K)| + |rot(K)| \leq -\chi(K)$.*

Proof: We want to apply the Bennequin inequality to a Legendrian knot K' in the complement of K (which is a tight manifold, since K is non-loose).¹³

We obtain K' modifying the knot K_ε used in Definition 3.1(i) to define the Thurston-Bennequin invariant so that it becomes homologically trivial in the complement of K . The modification will be performed locally, in a small tight ball, where the front diagrams of K and K_ε are two parallel line segments. The further procedure depends on the sign of $tb(K)$ as follows.

$tb(K) \leq 0$

Replace K_ε by K' as in Figure 22(a). (In particular, for $tb(K) = 0$ we take $K' = K_\varepsilon$.) Here K' is in fact Legendrian isotopic to K , therefore obviously $tb(K') = tb(K)$ and $rot(K') = rot(K)$.

$tb(K) > 0$

In this case, let K' be the knot depicted in Figure 22(b). By Propositions 3.4 and 3.6, $tb(K') = tb(K) - 2tb(K) = -tb(K)$ (since there are $4tb(K)$ newly added cusps) and $rot(K') = rot(K)$ (since there are equal numbers of ascending and descending cusps among the new ones).

Thus in both cases we have $rot(K') = rot(K)$ and

$$tb(K') = \begin{cases} tb(K) & \text{for } tb(K) \leq 0 \\ -tb(K) & \text{for } tb(K) > 0 \end{cases} = -|tb(K)|.$$

Moreover, since χ is a topological invariant, $\chi(K') = \chi(K)$. Therefore, by Theorem 3.3 for K' ,

$$-|tb(K)| + |rot(K)| \leq -\chi(K).$$

Proposition 5.4. *Let ξ be an overtwisted contact structure on S^3 , K a non-loose Legendrian unknot in ξ . Then $tb(K) > 0$ and $|rot(K)| < tb(K)$.*

Proof: Suppose $K = \partial D$ (D an embedded disk) is a Legendrian unknot in ξ and $tb(K) = 0$. Then the knot K' defined in the proof of Proposition 5.3 is in fact isotopic to K . On the other hand, K' is a Legendrian unknot in $S^3 \setminus D$. The complement of the disk D is homeomorphic to \mathbf{R}^3 , and tight (because K is non-loose). Thus we can consider K' as

¹³ A similar observation (though never explicitly expressed) must have prompted Etnyre and Ng to make the “final remark” in Section 6 in [10]: *any Legendrian knot that violates the Bennequin inequality is automatically loose*. This statement is not correct; Proposition 5.3 allows for non-loose knots violating the Bennequin inequality (in the $tb > 0$ case). Proposition 5.4 shows that this correction is essential.

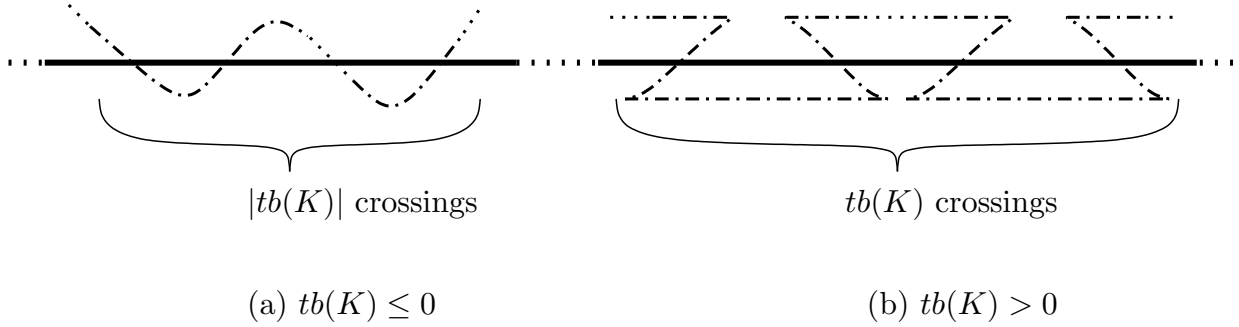


Figure 22: Construction of the knot K' in Proposition 5.3.

a Legendrian knot in the standard tight contact structure on \mathbf{R}^3 . Choose a tight ball in $S^3 \setminus D$ so that there is an overtwisted disk disjoint with it, and a Legendrian unknot K_0 in B with $tb(K_0) = tb(K')$, $rot(K_0) = rot(K')$. By the classification of Legendrian unknots given by Eliashberg and Fraser in [6] K_0 is Legendrian isotopic to K' , thus also to K . But K_0 is standard, while K is non-loose: a contradiction. \square

For a Legendrian knot K the pair of integers $(rot(K), tb(K))$ can be represented as a point in the plane (with integer coordinates of different parity). Then the values of invariants allowed (by Proposition 5.4) for non-loose **unknots** are contained in one quadrant of the plane (dark shading in Figure 23; the light shading denotes pairs (t, r) satisfying Proposition 5.3, but not Proposition 5.4). In fact, we only know the actual representants (non-loose unknots with given rotation and Thurston-Bennequin invariant) for points (rot, tb) on the boundary of this area (the black dots): those are the knots $\Gamma_{\pm 1, \mp n}$ (for any $n > 0$) defined in Example 2.3.

Proposition 5.5. *The knots $\Gamma_{m,n}$ with $mn < 0$ are non-loose.*

Proof: The proof is analogous to the proof of Proposition 4.9. We show that the complement of the knot $\Gamma_{m,n}$ is tight by embedding its universal cover into the standard tight \mathbf{R}^3 .

Let $\alpha = \arctan(m/n)$, so that $\text{pr}_C^{-1}(\Gamma_{m,n})$ lies in the plane $x = \alpha$. Then for $M = S^3 \setminus \Gamma_{m,n}$ we have $M = M_f \cup M_b$, where $M_f = \text{pr}_C([0, \alpha] \times [0, 1]^2) \setminus \Gamma_{m,n}$ and $M_b = \text{pr}_C([\alpha, 1] \times [0, 1]^2) \setminus \Gamma_{m,n}$. The universal cover \widetilde{M}_f is diffeomorphic to $H_m \times \mathbf{R}$, where H_m denotes a 2-dimensional disk with m boundary points p_1, \dots, p_m removed (and similarly $\widetilde{M}_b \simeq H_n \times \mathbf{R}$; the following argument applies to each of them).

The contact structure on \widetilde{M}_f extends to a contact structure on $\widetilde{M}_f \cup \{p_2\} \times \mathbf{R} \cup \dots \cup \{p_m\} \times \mathbf{R}$, isomorphic to the contact structure on M_0 used in the proof of Proposition 4.9. Therefore, we have a contact embedding $J : \widetilde{M}_f \rightarrow (\mathbf{R}^3, \zeta)$ with the boundary mapped into

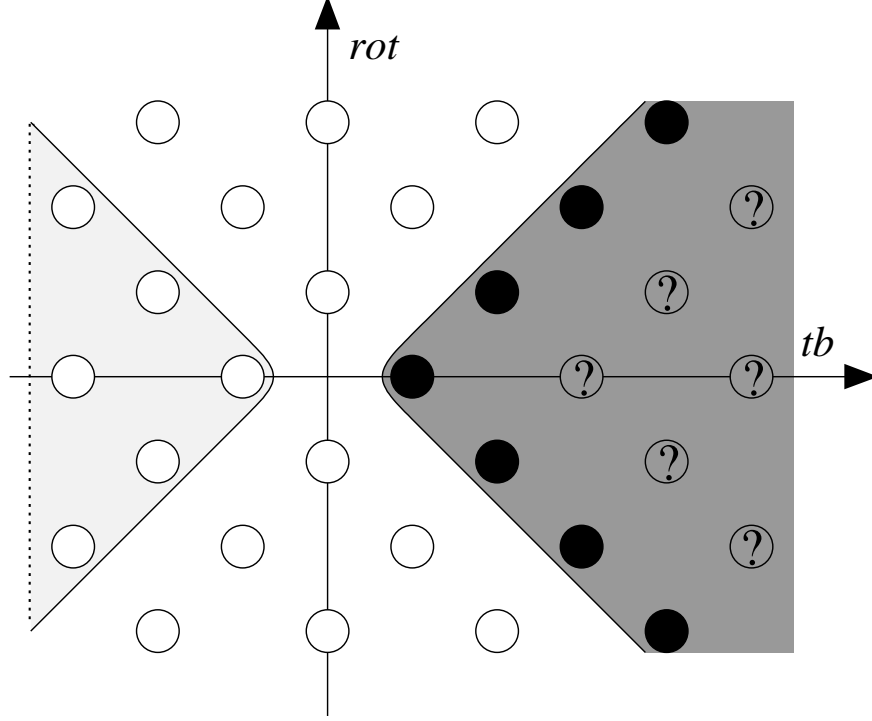


Figure 23: Non-loose unknots (known and potential).

the plane $x = 0$ (actually onto, except for the $m - 1$ lines $\{x = 0, z = z_i\}, i = 2, \dots, m\}$ which are “images” of $\{p_i\} \times \mathbf{R}$).

We want, however, to find an embedding whose image is contained in a proper subset of \mathbf{R}^3 , so that there is enough space left for other copies of \widetilde{M}_f and \widetilde{M}_b . It is well known that (\mathbf{R}^3, ζ) can be contactomorphically embedded into an arbitrarily small open subset of itself. Let $h : \mathbf{R}^3 \rightarrow \{x^2 + z^2 < C\}$ be such a contact embedding. We can assume that h maps the plane $x = 0$ into itself.

For our purposes, $h \circ J$ is better than J , but still not perfect, and needs further fine-tuning. Let $R : \widetilde{M}_f \rightarrow \widetilde{M}_f$ be the rotation by the angle $2\pi/m$, cyclically permuting the p_i ’s. Then $h \circ J \circ (R \circ J^{-1} \circ h \circ J)^{m-1}$ embeds \widetilde{M}_f into $H \times \mathbf{R}$, where H is a subset of the half-plane bounded by the line $x = 0$ and m arcs; see Figure 24 with $m = 3$.

Figure 25 shows the pattern of gluing together the pieces constructed in the described way. The flexibility in setting values of J on the boundary of \widetilde{M}_f which we enjoy in the early stages of this construction (cf. the proof of Lemma 4.2.1 in [4]) is sufficient to ensure that the embedding of \widetilde{M}_f and \widetilde{M}_b glue together in a compatible way to give an embedding of the whole \widetilde{M} .

Question 5.6. Let r, t be integers satisfying the conditions $r + t \equiv 1 \pmod{2}$, $t \geq 3$, $|r| \geq t - 3$. Does there exist a non-loose Legendrian unknot K with $rot(K) = r$ and $tb(K) = t$?

Of course, there do exist *loose* unknots for any given values of invariants (of different

parity, of course). This means that for some values there are (at least) two non-isotopic knots. For example, we list all that is known about Legendrian unknots K such that $rot(K) = 0$ and $tb(K) = 1$.

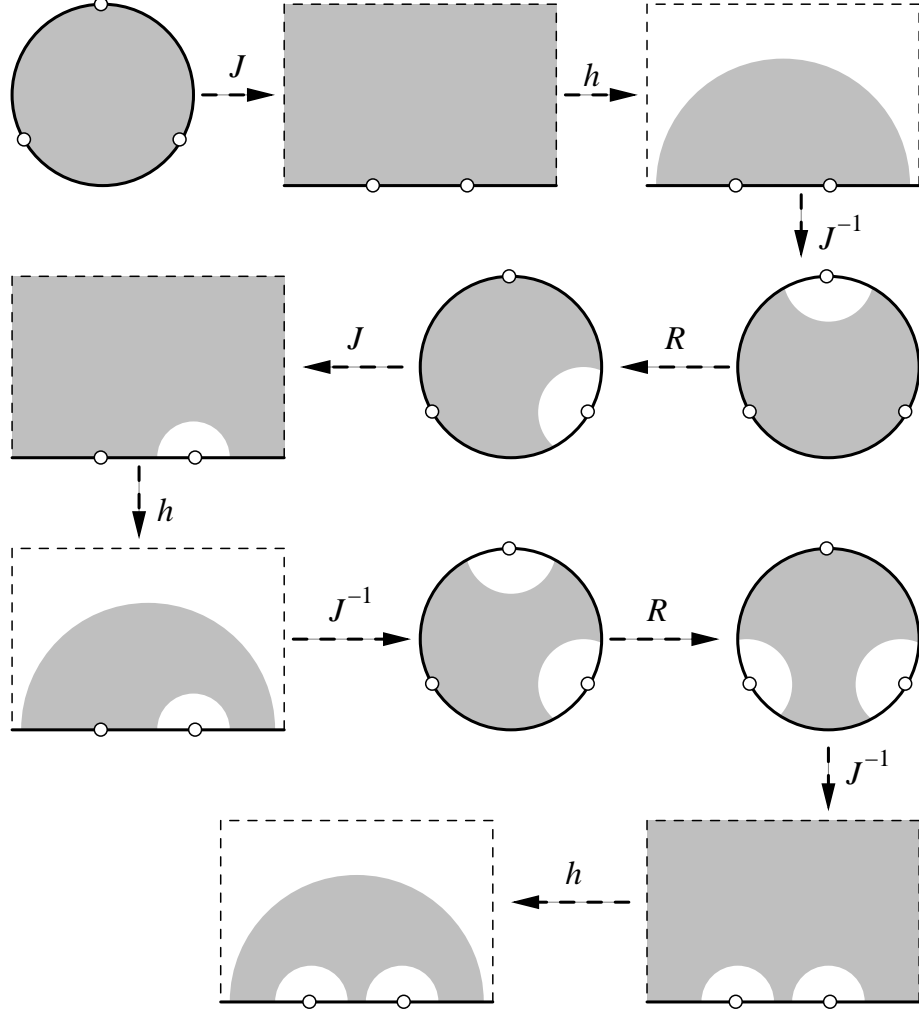


Figure 24: Constructing a building block for $\widetilde{M} \hookrightarrow \mathbf{R}^3$

Example 5.7. Consider the four Legendrian unknots of Figure 26 (each of them has $tb = 1$ and $rot = 0$):

- (i) $\Gamma_{0,1} \# \bar{\Gamma}_{0,1}$ and $\Gamma_{1,0} \# \bar{\Gamma}_{1,0}$ are loose, while $\Gamma_{1,1}$ and $\bar{\Gamma}_{1,1}$ are not, thus neither $\Gamma_{1,1}$ nor $\bar{\Gamma}_{1,1}$ is isotopic to $\Gamma_{0,1} \# \bar{\Gamma}_{0,1}$ or to $\Gamma_{1,0} \# \bar{\Gamma}_{1,0}$;
- (ii) it is not known whether $\Gamma_{0,1} \# \bar{\Gamma}_{0,1}$ and $\Gamma_{1,0} \# \bar{\Gamma}_{1,0}$ are isotopic;
- (iii) it is not known whether $\Gamma_{1,1}$ and $\bar{\Gamma}_{1,1}$ are isotopic;
- (iv) it is not known if there exist any other (non-isotopic) Legendrian unknots with the same values of invariants.

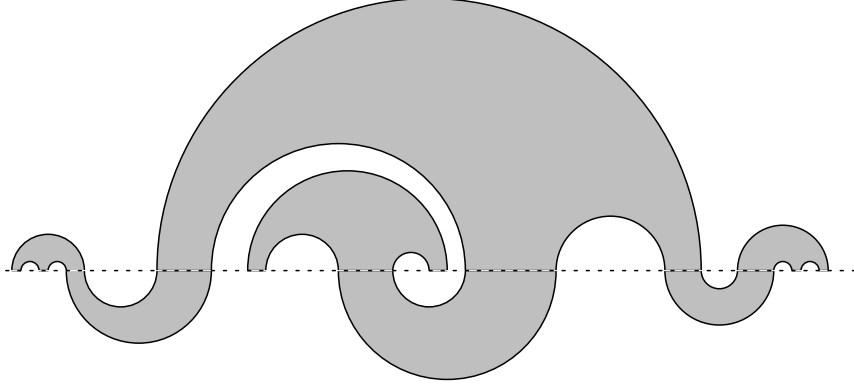


Figure 25: Gluing the building blocks together

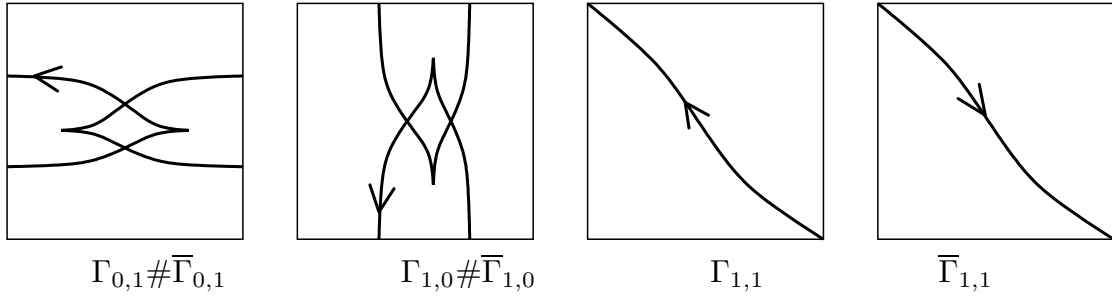


Figure 26: Legendrian knots with $rot = 0$ and $tb = 1$.

6 References

- [1] V. I. ARNOLD, *Mathematical Methods of Classical Mechanics*, vol. 60 of Graduate Texts in Mathematics, Springer-Verlag, 1978. Translated from the Russian by K. Vogtmann and A. Weinstein.
- [2] D. BENNEQUIN, *Entrelacements et équations de Pfaff*, Asterisque, 107–108 (1983), pp. 87–161.
- [3] Y. CHEKANOV, *Differential algebra of Legendrian links*, Invent. Math., 150 (2002), pp. 441–483.
- [4] K. DYMARA, *Legendrian knots in overtwisted contact structures on S^3* , Ann. Global Anal. Geom., 19 (2001), pp. 293–305.
- [5] Y. ELIASHBERG, *Classification of overtwisted contact structures on 3-manifolds*, Invent. Math., 98 (1989), pp. 623–637.
- [6] Y. ELIASHBERG AND M. FRASER, *Classification of topologically trivial Legendrian knots*, in Geometry, Topology and Dynamics, F. Lalonde, ed., no. 15 in CRM Proc. Lecture Notes, 1998, pp. 17–51.

- [7] J. B. ETNYRE, *Tight contact structures on lens spaces*, Commun. Contemp. Math., 2 (2000), pp. 559–577. Available also as [arXiv:math.DG/9812065](#).
- [8] J. B. ETNYRE AND K. HONDA, *On the non-existence of tight contact structures*, Ann. of Math. (2), 153 (2001), pp. 749–766. Available also as [arXiv:math.GT/9910115](#).
- [9] ———, *Knots and geometry II: Connected sums*. [arXiv:math.SG/0205310](#), 2002.
- [10] J. B. ETNYRE AND L. L. NG, *Problems in low dimensional contact topology*, in Topology and geometry of manifolds (Athens, GA, 2001), vol. 71 of Proc. Sympos. Pure Math., Amer. Math. Soc., Providence, RI, 2003, pp. 337–357. Available also at <http://www.math.upenn.edu/~etnyre/preprints/problems.ps.gz>.
- [11] M. FRASER, *Example of nonisotopic Legendrian curves not distinguished by the invariants tb and r* , Internat. Math. Res. Notices, (1996), pp. 923–928.
- [12] D. FUCHS AND S. TABACHNIKOV, *Invariants of Legendrian and transverse knots in the standard contact space*, Topology, 36 (1997), pp. 1025–1053.
- [13] J. W. GRAY, *Some global properties of contact structures*, Ann. of Math. (2), 69 (1959), pp. 421–450.
- [14] K. HONDA, *On the classification of tight contact structures I*, Geom. Topol., 4 (2000), pp. 309–368. Available also as [arXiv:math.DG/9910127](#).
- [15] K. HONDA, *On the classification of tight contact structures II*, J. Differential Geom., 55 (2000), pp. 83–143.
- [16] L. L. NG, *Computable Legendrian invariants*. [arXiv:math.GT/0011265](#), 2000.
- [17] L. L. NG, *The Legendrian satellite construction*. [arXiv:math.GT/0112105](#), 2001.
- [18] J. ŚWIĄTKOWSKI, *On the isotopy of Legendrian knots*, Ann. Global Anal. Geom., 10 (1992), pp. 195–207.
- [19] V. TCHERNOV, *Framed knots in 3-manifolds and affine self-linking numbers*. [arXiv:math.GT/0105139](#), 2001. To appear in J. Knot Theory Ramifications, 2005.
- [20] ———, *Vassiliev invariants of Legendrian, transverse, and framed knots in contact three-manifolds*, Topology, 42 (2003), pp. 1–33.